Journal of Cerebral Blood Flow & Metabolism (2009), 1–11

www.jcbfm.com

Measurement of density and affinity for dopamine D_2 receptors by a single positron emission tomography scan with multiple injections of [^{11}C]raclopride

Yoko Ikoma[1,2], Hiroshi Watabe[1], Takuya Hayashi[1], Yoshinori Miyake[1], Noboru Teramoto[1], Kotaro Minato[2] and Hidehiro Iida[1]

[1]*Department of Investigative Radiology, National Cardiovascular Center Research Institute, Osaka, Japan;* [2]*Biomedical Imaging and Informatics, Graduate School of Information Science, Nara Institute of Science and Technology, Nara, Japan*

Positron emission tomography (PET) with [^{11}C]raclopride has been used to investigate the density (B_{max}) and affinity (K_d) of dopamine D_2 receptors related to several neurological and psychiatric disorders. However, in assessing the B_{max} and K_d, multiple PET scans are necessary under variable specific activities of administered [^{11}C]raclopride, resulting in a long study period and unexpected physiological variations. In this paper, we have developed a method of multiple-injection graphical analysis (MI-GA) that provides the B_{max} and K_d values from a single PET scan with three sequential injections of [^{11}C]raclopride, and we validated the proposed method by performing numerous simulations and PET studies on monkeys. In the simulations, the three-injection protocol was designed according to prior knowledge of the receptor kinetics, and the errors of B_{max} and K_d estimated by MI-GA were analyzed. Simulations showed that our method could support the calculation of B_{max} and K_d, despite a slight overestimation compared with the true magnitudes. In monkey studies, we could calculate the B_{max} and K_d of diseased or normal striatum in a 150 mins scan with the three-injection protocol of [^{11}C]raclopride. Estimated B_{max} and K_d values of D_2 receptors in normal or partially dopamine-depleted striatum were comparable to the previously reported values.
Journal of Cerebral Blood Flow & Metabolism advance online publication, 11 November 2009; doi:10.1038/jcbfm.2009.239

Keywords: [^{11}C]raclopride; dopamine D_2 receptors; graphical analysis; multiple injections; positron emission tomography

Introduction

Positron emission tomography (PET) with [^{11}C]raclopride has been widely used to investigate the availability of striatal dopamine D_2 receptors *in vivo* (Farde *et al*, 1985; Köhler *et al*, 1985; Hall *et al*, 1988). A number of postmortem studies have shown that the abundance of dopamine D_2 receptor is elevated in striatum samples from untreated patients with Parkinson's disease (Guttman and Seeman, 1985; Seeman *et al*, 1987) and in schizophrenic patients who had never taken antipsychotics (Cross *et al*, 1981; Joyce *et al*, 1988). The PET measurements have made it possible to quantify *in vivo* the density and apparent affinity of receptors by systematically varying the specific activity (or mass) of an administered radioligand (see for example, Farde *et al*, 1986). A study of Parkinson's disease by Rinne *et al* (1995) with *in vivo* PET showed increased density and unchanged affinity of dopamine D_2 receptors in the putamen in comparison with healthy controls. In corresponding studies of schizophrenia, early findings with [^{11}C]*N*-methylspiperone indicated elevated D_2 binding, which was not replicated in some subsequent studies with [^{11}C]raclopride (Wong *et al*, 1986; Farde *et al*, 1987, 1990). Dysfunction of dopamine receptors has also been suggested in other neurodegenerative or psychiatric diseases (e.g., multiple-system atrophy, progressive supranuclear palsy, and attention-deficit hyperactivity disorders); however, there have been only a few studies that

Correspondence: Dr H Watabe, Department of Investigative Radiology, National Cardiovascular Center Research Institute, 5-7-1, Fujishirodai, Suita, Osaka 565-8565, Japan.
E-mail: watabe@ri.ncvc.go.jp
Received 11 September 2009; revised 13 October 2009; accepted 19 October 2009

examined receptor function directly related to density and affinity. This might be due to the inherent difficulty in measuring absolute receptor abundance based on PET recordings.

In PET scans, to determine the density and affinity of receptors directly as parameters of kinetic model, it is necessary to apply a compartmental analysis based on a two-tissue compartment five-parameter model including density of receptors B_{max} (pmol/mL), bimolecular association rate constant k_{on} (mL/pmol/min), and unimolecular dissociation rate constant k_{off} (min^{-1}) (Farde *et al*, 1989). However, since data from a single PET scan are not enough to determine the B_{max} and k_{on} individually, multiple PET scans should be taken with different molar amounts of injected ligand. In addition, model parameters are estimated by a nonlinear least squares fitting with the metabolite-corrected plasma input function, so the solutions are often unstable and sensitive to statistical noise, and invasive arterial sampling is required to use this method.

Farde *et al* (1986, 1989) determined the value of B_{max} and apparent affinity K_d ($=k_{off}/k_{on}$) by a graphical analysis using a time-activity curve (TAC) of the specifically bound target region and a reference region where specific bindings are negligible. In this method, the ratio of specific bound and free ligand concentrations at the equilibrium state are plotted versus the concentration of specific bound ligand, and B_{max} and K_d are estimated from the slope and intercept of the regression line. Other groups also used the value of distribution volume ratio − 1 estimated from the graphical analysis of Logan *et al* (1996), instead of the ratios of specific bound and free concentration, to obtain stable values of the *y*-axis quantity (Logan *et al*, 1997; Doudet and Holden, 2003; Doudet *et al*, 2003). These methods are practical, because they do not require arterial blood sampling, and their respective estimation processes are easy to carry out. However, to estimate the regression line of a graphical plot, multiple PET scans (at least two or three) are required under variable molar amounts of administered ligand, so scans have been performed on separate days. Even in quantitative PET scans, the separate day protocol may suffer from interday or intraday variations in physiologic conditions, such as cerebral blood pressure, flow, and receptor bindings, which may affect the accuracy of the estimates.

We developed a method, called the multiple-injection simplified reference tissue model (MI-SRTM), to measure the change in binding potential ($BP_{ND}=k_3/k_4$ (Mintun *et al*, 1984)) of dopamine D_2 receptors from a single session of PET scanning with multiple injections of [^{11}C]raclopride (Watabe *et al*, 2006; Ikoma *et al*, 2009), and we showed that this method could detect the change in BP_{ND} because of an increase in mass of administered [^{11}C]raclopride in a short scanning period, which is a prerequisite for measuring the saturation binding parameters as steady state. In this study, we extend our earlier report for estimating B_{max} and K_d from a single session of PET scanning with triple injections of [^{11}C]raclopride using MI-SRTM and the graphical analysis, and we validated the proposed method by performing numerous simulations and studies on monkeys using PET and [^{11}C]raclopride.

Materials and methods

Theory

Graphical Analysis with a Reference Region for Estimation of Density and Affinity: Graphical analysis based on the Scatchard plot (Scatchard, 1949) has been used to estimate the values of B_{max} and K_d from as series of PET recordings with various molar amounts of administered ligand (Farde *et al*, 1986). In brief, the ratios (B/F) of specific bound ligand concentration (B [pmol/mL]) and free ligand concentration (F [pmol/mL]) at equilibrium are plotted versus B. In this plot, the slope and *x*-intercept represent $-1/K_d$ and B_{max}, respectively. In general, for graphical analysis without arterial blood sampling, the total radioligand concentration in the reference region (C_r [Bq/mL]), where specific bindings are negligible, is used as an estimate of the free radioligand concentration in the target region (C_f [Bq/mL]), that is $C_f^{ref}=C_r$, and the specific binding radioligand concentration in the target region (C_b [Bq/mL]) is defined as radioactivity in the target region (C_t [Bq/mL]) reduced with C_r, that is $C_b^{ref}=C_t-C_r$ (Figure 1). The radioactivity concentrations of C_f^{ref} and C_b^{ref}, at the point in time when dC_b^{ref}/dt is 0 (T_{eq}), are divided by a specific activity of the administered ligand, and used as F and B at the transient equilibrium in the graphical analysis

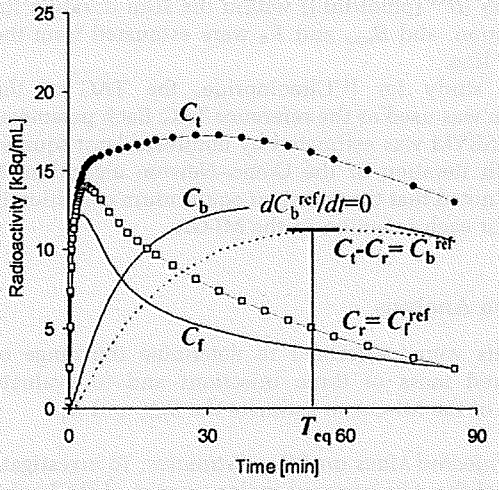

Figure 1 An example of simulated TACs for the striatum (C_t), free (C_f), and specific bound (C_b) concentrations in the striatum, the cerebellum used as a reference region (C_r) and bound concentration in the striatum estimated using a reference region ($C_b^{ref}=C_t-C_r$) with $K_1=0.033$, $K_1/k_2=0.59$, $k_{on}=0.0033$, $B_{max}=25.7$, $k_4=0.034$ for the striatum, and $K_1=0.034$, $K_1/k_2=0.36$, $k_3=0.022$, $k_4=0.034$ for the cerebellum. The time point of $dC_b^{ref}/dt=0$ (T_{eq}) is considered the transient equilibrium, and bound concentration at the equilibrium (B^{ref}) is obtained from the radioactivity concentration of C_b^{ref} at T_{eq}.

(Farde *et al*, 1989). In our study, we use the nomenclature B^{ref} and F^{ref} to represent the concentrations otherwise known as B and F. The value of the y axis, B^{ref}/F^{ref}, is sometimes replaced by the binding potential estimated by the graphical analysis of Logan *et al* (1996) or some other method (Logan *et al*, 1997; Doudet and Holden, 2003; Doudet *et al*, 2003).

Multiple-Injection Simplified Reference Tissue Model for Estimation of Binding Potential: A simplified reference tissue model (SRTM) can provide three parameters (R_1, k_2, BP_{ND}) without invasive arterial blood sampling by using a TAC of the reference region (Lammertsma and Hume, 1996). The MI-SRTM extended this SRTM for sequential multiple injections in a single session of PET scanning by taking into account the residual radioactivity in the target tissue at the time of each injection. As such, the magnitude of BP_{ND} for the ith injection is described in the following terms (Ikoma *et al*, 2009):

$$C_{ti}(t) = R_{1i}C_{ri}(t) + \left(k_{2i} - \frac{R_{1i}k_{2i}}{1+BP_{NDi}}\right)e^{-\frac{k_{2i}}{1+BP_{NDi}}t} \otimes C_{ri}(t) + (C_{ti}(0) - R_{1i}C_{ri}(0))e^{-\frac{k_{2i}}{1+BP_{NDi}}t} \quad (1)$$

where C_{ti} and C_{ri} are the radioactivity concentrations in the target and reference region, respectively, and t is the time from the start of the ith injection.

Multiple-Injection Graphical Analysis for Estimation of Density and Affinity: The conventional graphical analysis was applied to the B_{max} and K_d estimations with the multiple-injection approach. In this multiple-injection graphical analysis (MI-GA), the BP_{ND} calculated for each injection using MI-SRTM was plotted as a function of the concentration of specific bound raclopride at the transient equilibrium (B^{ref} [pmol/mL]) within the scan duration for each injection, and B_{max} and K_d were estimated from the regression line.

In this study for [^{11}C]raclopride, the TAC of the cerebellum was used as the reference TAC. Each parameter in the MI-SRTM was estimated by nonlinear least squares fitting with iteration of the Gauss–Newton algorithm. It should be noted that the transient equilibrium condition is required for each injection in the MI-GA.

Simulation Analysis

Simulations were performed to determine the range of administered mass of three injections and to evaluate feasibility of the MI-GA to estimate the B_{max} and K_d.

Effect of Injected Mass on BP_{ND} Estimates: To investigate the effect of the administered molar amount of [^{11}C]raclopride on BP_{ND} estimates and to determine the molar amount of three injections for monkey studies, a relationship between BP_{ND} and B^{ref} was obtained by a computer simulation. Noiseless TACs of the striatum and cerebellum were generated with a measured plasma TAC and assumed parameter values derived from measurements taken from the monkey studies. The TAC of the cerebellum was simulated with a conventional two-tissue compartment four-parameter model with assumed parameter values obtained earlier in our monkey studies: $K_1 = 0.034$ (mL/mL/min) $K_1/k_2 = 0.36$, $k_3 = 0.022$ (min^{-1}), $k_4 = 0.034$ (min^{-1}). Meanwhile, the TAC of the striatum was simulated with a two-tissue compartment five-parameter model expressed as Equation (2) by solving these differential equations with the numerical analysis of fourth-order Runge–Kutta method with assumed parameter values $K_1 = 0.033$ (mL/mL/min), $K_1/k_2 = 0.59$, $k_{on} = 0.0033$ (mL/pmol/min), $B_{max} = 25.7$ (pmol/mL), $k_4 = 0.026$ (min^{-1}), and SA = 37 (GBq/μmol):

$$\begin{aligned} \frac{dC_f}{dt} &= K_1C_p(t) - \left(k_2 + k_3'(t)\right)C_f(t) + k_4C_b(t) \\ \frac{dC_b}{dt} &= k_3'(t)C_f(t) - k_4C_b(t) \\ k_3'(t) &= k_{on}\left(B_{max} - \frac{C_b(t)}{SA}\right) \end{aligned} \quad (2)$$

where C_f and C_b are the concentrations of radioactivity for free and specifically bound [^{11}C]raclopride in tissue, respectively; and SA is the specific activity of administered [^{11}C]raclopride.

As reference, the relationships between B^{ref} and BP_{ND} or B^{ref}/F^{ref} were investigated in the case of a single injection of [^{11}C]raclopride by varying injected mass. TACs of the striatum and cerebellum for the single injection with a 50 mins scan were generated using the measured plasma TAC of a single injection in which the input plasma TAC was amplified, such that the corresponding mass increased from 1 to 500 nmol per injection. In each simulated TAC, BP_{ND} values were estimated by the SRTM, and then, B^{ref}/F^{ref} and B^{ref} were calculated by the transient equilibrium with the cerebellum TAC.

Next, TACs of the striatum and cerebellum for three injections at 50 mins intervals were generated using the plasma TAC of three sequential injections in which the input plasma TAC was amplified so that the mass of the first and second injections would be 1.5 and 10 nmol/kg, and the mass of the third injection would be 1.5 to 150 nmol/kg. In each simulated TAC, BP_{ND} values were estimated by the MI-SRTM, and B^{ref}/F^{ref} and B^{ref} for the third injection was calculated by the transient equilibrium with the cerebellum TAC. The relationships between B^{ref} and BP_{ND} or B^{ref}/F^{ref} for the third injection were investigated, and compared with that for the single injection.

Estimation of B_{max} and K_d Values by the Multiple-Injection Graphical Analysis: The reliability of B_{max} and K_d estimates by the graphical analysis was investigated for the proposed sequential multiple-injection approach (single PET scan) and compared with that for the conventional nonsequential approach (three PET scans on different days, such that no residual mass remained). Noiseless TACs of the striatum and cerebellum were simulated using assumed parameters of the two-tissue compartment model mentioned above and the plasma input function for three injections in which the magnitude of each 'virtual' input function was adjusted so that the injection mass would be 1.5, 10, or 30 nmol/kg determined from the simulation study mentioned above, with 50 mins intervals as reported

by Ikoma *et al* (2009). In the striatum TACs, B_{max} values were varied from 10 to 50 pmol/mL at 5 pmol/mL intervals with other parameters fixed ($K_d = 7.9$ pmol/mL), or K_d was varied from 3 to 15 at 2 pmol/mL intervals by changing k_{on} with other parameters fixed ($B_{max} = 25.7$ pmol/mL). For each TAC, B_{max} and K_d were estimated by the MI-GA from three points obtained by MI-SRTM for the single PET scan approach and they were estimated by the graphical analysis from three points obtained by the conventional SRTM for the three PET scan approach. Then, estimates were compared with the true values. In the single PET scan approach, B_{max} and K_d were also estimated without reference TAC by the MI-GA from three points of BP_{ND} and B obtained by the two-tissue compartment four-parameter model with the plasma input function shown in the Appendix.

Analysis of Monkey Studies

PET studies were performed on three cynomolgus macaques (weight 6.9 ± 2.1 kg) with the multiple-injection approach. One animal (monN) was a healthy monkey aged 5 years, and the others had a syndrome acquired Parkinsonism. Of these, one (monUP, aged 7 years) had hemiparkinsonism induced by injecting the selective neurotoxin, *N*-methyl-4-pheny1-1,2,3,6-tetrahydropyridine (MPTP) (0.4 mg/kg) into the right carotid artery (Bankiewicz *et al*, 1986), whereas the other (monBP, aged 5 years) had bilateral Parkinsonism induced by injecting MPTP (0.4 mg/kg) intravenously and intermittently (twice a week for a total of 14 injections) (Takagi *et al*, 2005). Each Parkinsonian animal showed typical Parkinsonian symptoms in the limbs (motor slowness, tremor) unilaterally or bilaterally. The PET scan was performed after the symptom reaching stable (6 months after the first injection of MPTP). Anesthesia was induced with ketamine (8.4 mg/kg, intramuscularly) and xylazine (1.7 mg/kg, intramuscularly) and maintained by intravenous propofol (6 mg/kg/h) and vecuronium (0.02 mg/kg/h) during the scan. The monkeys were maintained and handled in accordance with guidelines for animal research on Human Care and Use of Laboratory Animals (Rockville, National Institutes of Health/Office for Protection from Research Risks, 1996). The study protocol was approved by the Subcommittee for Laboratory Animal Welfare of the National Cardiovascular Center.

After the synthesis of [^{11}C]raclopride, nonradioactive raclopride was added so that targeted molar amount of raclopride would be administered for three injections (1.5, 10, and 30 nmol/kg); this was done by dividing the [^{11}C]raclopride diluted by nonradioactive raclopride into three portions with different volumes, containing the intended masses of raclopride. For the first injection, 1.9 ± 0.16 nmol/kg (57.0 ± 5.7 MBq) of [^{11}C]raclopride was administered by a bolus injection at the beginning of the scan. Fifty minutes later, the second [^{11}C]raclopride injection, 11.1 ± 0.56 nmol/kg (60.4 ± 8.8 MBq at the time of second injection) was administered by a bolus, and 50 mins after that, a bolus of 31.1 ± 2.1 nmol/kg (30.8 ± 4.4 MBq at the time of third injection) of [^{11}C]raclopride was administered again. Data were acquired for 150 mins (10 secs × 18, 30 secs × 6, 120 secs × 7, 300 secs × 6; total 50 mins for each injection). The specific radioactivity was 4.7 ± 2.2 GBq/μmol at the time of the first injection.

PET scans were performed using a PCA-2000A positron scanner (Toshiba Medical Systems Corporation, Otawara, Japan) that provides 47 planes and a 16.2 cm axial field-of-view. The transaxial and axial spatial resolution of the PET scanner were 6.3 and 4.7 mm full width at half maximum (Herzog *et al*, 2004). A transmission scan with a 3-rod source of ^{68}Ge-^{68}Ga was performed for 20 mins for attenuation correction before the administration of [^{11}C]raclopride. Radioactivity was measured in the three-dimensional mode and the data were reconstructed by a filtered back-projection using a Gaussian filter (3 mm of full width at half maximum). Region-of-interests (ROIs) were defined manually over the left and right striatum and cerebellum for PET images, and the radioactivity concentrations in these regions were obtained. For the left and right striatum, R_1, k_2, and BP_{ND} for each injection were estimated by the MI-SRTM. In addition, parametric images were generated, estimating each parameter voxel by voxel, using the MI-SRTM with a basis function method in which the model Equation (1) was solved using linear least squares for a set of basis functions, which enables the incorporation of parameter bounds (Gunn *et al*, 1997; Ikoma *et al*, 2009). B_{max} and K_d were estimated by the MI-GA from these BP_{ND} values of left and right striatum for three injections.

In the unilateral Parkinsonian animal, three PET scans with conventional single injection with different masses of [^{11}C]raclopride were also performed for comparison with results by the multiple-injection single PET scan approach. A PET scan with a bolus injection of 2.1 nmol/kg (50.6 MBq), 11.3 nmol/kg (60.4 MBq), or 31.1 nmol/kg (30.8 MBq) of [^{11}C]raclopride was obtained on separate days. PET data were acquired for 50 mins with the same protocol as the single PET scan approach. The values of R_1, k_2, and BP_{ND} were estimated by the SRTM, and B_{max} and K_d were estimated by the conventional graphical analysis.

Results

Simulation Study

Effect of Injected Mass on BP_{ND} Estimates: In the simulations, the value of BP_{ND}, estimated by the MI-SRTM, decreased as injected molar amount of raclopride increased, that is, concentration of bound raclopride became larger. The relationship between BP_{ND} and B^{ref} had a good linear correlation to some extent; however, it did not remain linear for large B^{ref} (Figure 2A). The regression line where $B^{ref} < 20$ pmol/mL was $BP_{ND} = -0.091B^{ref} + 2.4$, $R^2 = 0.997$ for the first injection. In the relationship between BP_{ND} and B^{ref}, BP_{ND} values of the third injection were higher than those of the first injection when B^{ref} was lower than 20 pmol/mL. The ratio B^{ref}/F^{ref} was almost the same as the BP_{ND} estimated by MI-SRTM, though it was a little smaller when B^{ref} was lower than 5 pmol/mL (Figure 2B).

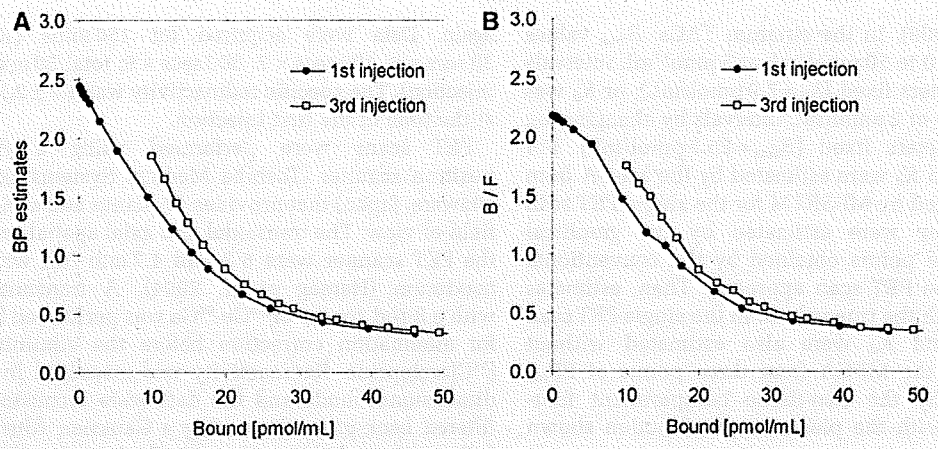

Figure 2 Relationship between specifically bound concentration and BP_{ND} **(A)** or B^{ref}/F^{ref} **(B)** estimates for the first and third injection in the simulations.

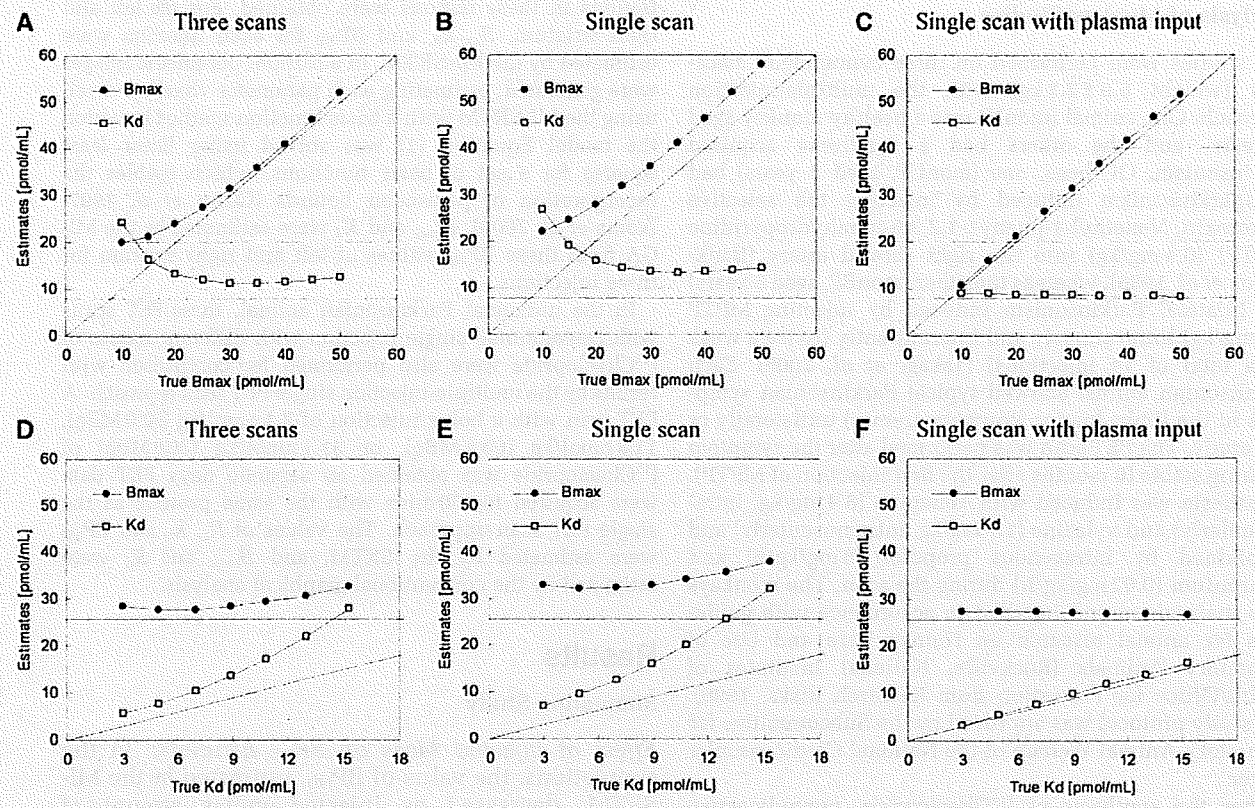

Figure 3 Relationships between estimates and true values of B_{max} and K_d for simulated TACs with various B_{max} and fixed K_d **(A–C)** and with various K_d and fixed B_{max} **(D–F)** by the three PET scan approach **(A, D)**, multiple-injection single PET scan approach **(B, E)**, and single PET scan approach with the plasma input function **(C, F)**.

Estimation of B_{max} and K_d Values by the Multiple-Injection Graphical Analysis: The TACs were calculated for a range of possible B_{max} and K_d values, and the relationship between true and estimated B_{max} or K_d values was investigated for conventional three PET scan and the proposed single PET scan approaches. When B_{max} was varied, B_{max} and K_d were overestimated compared with the true values in both three PET scan and single PET scan approaches (Figures 3A and 3B). However, a good correlation was observed between true and estimated B_{max}, and there was little variation in estimated K_d when B_{max} was set higher than 20 pmol/mL. Similarly, when K_d was varied, although K_d and B_{max} were overestimated in both approaches, there was a good correlation between true and estimated K_d, and estimated B_{max} was constant (Figures 3D and 3E). In both cases, B_{max} and K_d estimates in the single

PET scan approach were higher than those in the three PET scan approach. In the TAC simulated with $B_{max}=25.7$ and $K_d=7.0$, estimated B_{max} and K_d were 27.8 and 10.5, respectively, in the three PET scan approach, and 32.3 and 12.6, respectively, in the single PET scan approach. In contrast to these approaches with the reference TAC, the overestimation of B_{max} and K_d was scarcely observed in the MI-GA with the plasma input function (Figures 3C and 3F).

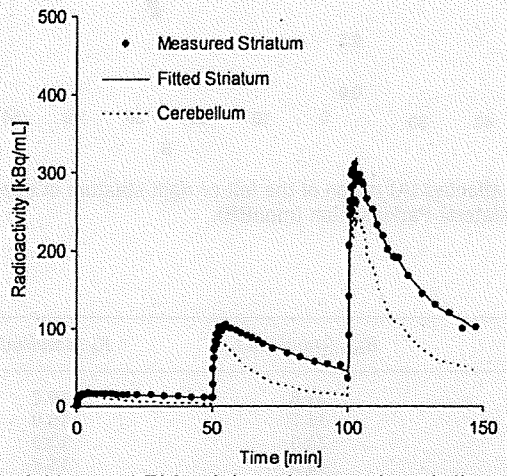

Figure 4 Measured TACs of the striatum and cerebellum and a fitted curve for the striatum using MI-SRTM in the monkey study by a single scan with sequential three injections of [^{11}C]raclopride.

Monkey Studies

Typical examples of TACs for the striatum and the cerebellum in the multiple-injection study are shown in Figure 4, and the parametric images of BP_{ND} for the first, second, and third injection, and images of B_{max} and K_d for the voxels in which BP_{ND1} was higher than 1.5 are shown in Figure 5. The estimated BP_{ND} decreased as the injected molar amount of [^{11}C]raclopride became larger in the second or third injection. Estimated BP_{ND1}, BP_{ND2}, and BP_{ND3} values were 2.3, 1.4, and 0.74, respectively, in the left striatum, and 2.6, 1.9, and 0.87, respectively, in the right striatum. The reduction in BP_{ND} was also observed in the parametric images.

The plots of MI-GA are shown in Figure 6. Plots of MI-GA for each of three animals were on the line, and B_{max} and K_d could be estimated as summarized in Table 1. Using the single scan approach for the hemiparkinsonian animal, B_{max} was 42.3 pmol/mL and K_d was 15.2 pmol/mL in the affected (right) striatum, and B_{max} was 32.3 pmol/mL and K_d was 13.0 pmol/mL in the contralateral (left) normal striatum. Corresponding estimates for the three scan approach were $B_{max}=36.4$ and $K_d=13.3$ pmol/mL in the right striatum and $B_{max}=29.2$ and $K_d=11.6$ pmol/mL in the

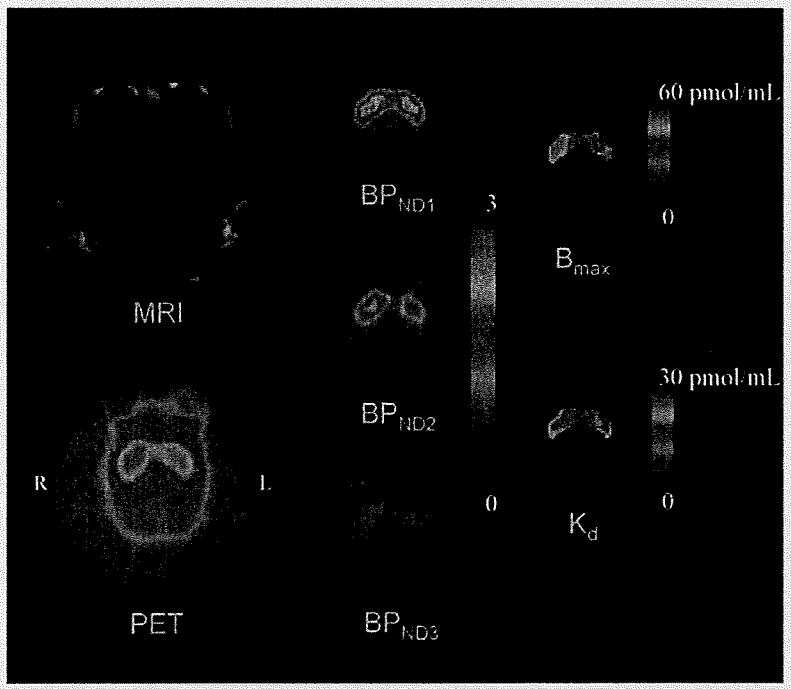

Figure 5 MRI and PET summation image (left) and parametric images of BP_{ND} for the first, second, and third injection (center) and parametric images of B_{max} and K_d for the voxels in which BP_{ND1} is higher than 1.5 (right) in the unilateral Parkinsonian (monUP) monkey study by a single scan with three sequential injections of [^{11}C]raclopride. Although ROI analysis disclosed higher B_{max} values in the MPTP-infused side of the striatum, the parametric image showed more evident increase of B_{max} in the dorsal and posterior parts of the striatum.

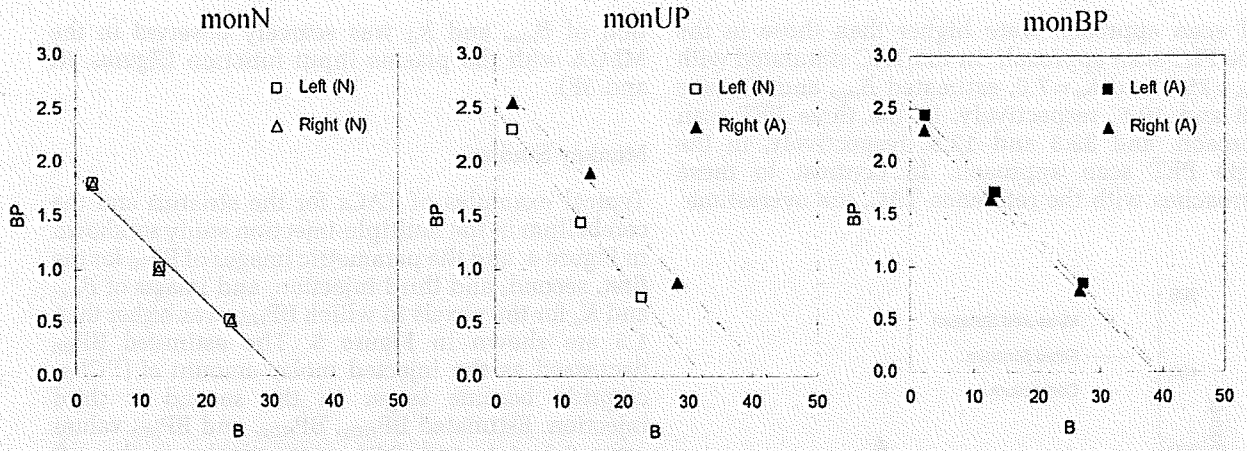

Figure 6 Single-scan, multiple-injection graphical analysis for normal (N) or affected (A) region of the left or right striatum in three monkeys that were normal (monN), unilateral Parkinsonian (monUP), and bilateral Parkinsonian (monBP).

Table 1 Estimated B_{max} and K_d values in three monkey studies

Scan protocol	*Subject*	*Region*	*Diagnosis*	B_{max} *(pmol/mL)*	K_d *(pmol/mL)*
Single scan	monN	L	N	31.8	16.7
		R	N	31.7	16.9
	monUP	L	N	32.3	13.0
		R	A	42.3	15.2
	monBP	L	A	39.6	15.4
		R	A	38.7	15.9
Three scans	monUP	L	N	29.2	11.6
		R	A	36.4	13.3

L, left striatum; R, right striatum; N, normal striatum; A, affected striatum.

left striatum. Both B_{max} and K_d of the single PET scan approach were slightly higher than those of the three PET scan approach. However, importantly, both approaches found that B_{max} in the affected striatum was higher than that in the normal striatum. The bilateral Parkinsonian animal showed B_{max} values of left = 39.6 pmol/mL, right = 38.7 pmol/mL, both of which were higher than those of the striatum of the normal animal or the normal striatum of the unilateral animal, but were very close to the affected striatum of the unilateral animal. The K_d values of the bilateral animal were not so different from other striatums.

Discussion

Density and Affinity Determination by Graphical Analysis with the Reference Region

In the graphical analysis for PET receptor studies, the values of B_{max} and K_d were estimated from the relationship between the ratio of bound to free concentrations and bound concentration at the time of transient equilibrium, using the TAC of the reference region (Farde *et al*, 1986). Some groups have used the value estimated from the distribution volume ratio − 1, instead of the B^{ref}/F^{ref} value of the y axis, because the values of B^{ref}/F^{ref} could change considerably with small changes in the time point of the transient equilibrium T_{eq} determined as the maximum C_b^{ref} (Logan *et al*, 1997; Doudet and Holden, 2003; Doudet *et al*, 2003). Distribution volume ratio or BP_{ND} is estimated from the kinetic analysis with TACs of target and reference regions, so it is not affected by the error of estimated T_{eq}. On the other hand, the value of $k'_3(t)$ in Equation (2) varies according to the concentration of bound raclopride, and estimates of BP_{ND} are considered to be an averaged value of specific binding over time, which is influenced by the dynamics of the free and bound raclopride. Despite this, in our simulation study of [^{11}C]raclopride, there was little difference between B^{ref}/F^{ref} and BP_{ND} estimated by the SRTM, and both had a linear correlation with B^{ref} (Figure 2). However, B^{ref}/F^{ref} became smaller than BP_{ND} and deviated from the linear relationship between B^{ref}/F^{ref} and B^{ref} in the region with low B^{ref} (Figure 2), especially for the TACs with high B_{max}. This may be a result of imperfect attainment of the transient equilibrium within the 50 mins scan duration for the TAC with high binding. There was little effect of the error of B^{ref} for the graphical analysis, in which B^{ref} varied widely among three injections, whereas the error of B^{ref}/F^{ref}

because of nonachievement of transient equilibrium had much effect on the graphical analysis as compared with BP_{ND}. Therefore, we estimated B_{max} and K_d by the graphical analysis with the relationship between BP_{ND} and B^{ref}.

In the simulations with various injected masses of [^{11}C]raclopride, it was shown that the relationship between BP_{ND} and B^{ref} became linear to some extent. However, BP_{ND} deviated from the linear relationship and approached a nonzero value when B^{ref} became larger (Figure 2). Therefore, in the B_{max} and K_d estimation by the graphical analysis with the reference TAC, points must be plotted within the range of the linear relation. As the relationship between BP_{ND} and B estimated from C_b using the plasma input function, without the reference TAC, remained linear even when B became large and the estimated BP_{ND} approached 0 (data not shown), this apparent saturation seemed to be owing to the reference region. Strictly speaking, the time course of free radioligand C_f is different from that of the reference region C_r (Figure 1) and C_f changes according to the specific binding that was affected by k_{on}, B_{max}, or administered mass of raclopride as pointed out by Ito *et al* (1998). Therefore, the time of the transient equilibrium estimated using C_b^{ref} was different from that estimated using C_b, and B^{ref} was often different as well. In addition, the value of BP_{ND} estimated by SRTM was lower than the BP_{ND} estimated from the two-tissue compartment model with the plasma input function.

This difference between the target and reference TAC affected the B_{max} and K_d estimates as well. In the simulated TACs with various B_{max} or K_d values, the B_{max} and K_d were overestimated compared with the true values even in the conventional three PET scan approach (Figure 3). On the other hand, the overestimation was not observed when B_{max} and K_d were estimated by the graphical analysis using C_f and C_b without the reference TAC (Figure 3), demonstrating that graphical analysis could determine B_{max} and K_d precisely if C_b were obtained correctly. However, the free and bound concentrations in the target region cannot be distinguished from the total concentration measured by PET scanning without arterial blood sampling, and in practical PET data, estimation of rate constants with the plasma input function is unstable and impractical. Therefore, in the usual graphical analysis, the TAC of reference region is used as the free radioligand concentration in the target region (Farde *et al*, 1989). The effect of the reference TAC on B_{max} and K_d estimates depends on the kinetics of the tracer in each region, which depends in turn on the particular tracers and species. In the simulated TACs of monkeys with [^{11}C]raclopride, there was a good correlation between true and estimated K_d or B_{max}, though estimates were biased. Therefore, we concluded the graphical analysis with reference TAC is practical for [^{11}C]raclopride studies, because it can detect the value of B_{max} or K_d in neurological or psychiatric disorders without arterial blood sampling.

Estimated Density and Affinity by the Multiple-Injection Approach

We applied the multiple-injection approach to the graphical analysis for B_{max} and K_d determination in an effort to shorten the total duration of the scanning protocol, and to obviate the need for several radiosyntheses for each animal. From the relationship between the BP_{ND} estimates and injected mass in the simulation study (Figure 2), the molar amounts of three injections were set as 1.5, 10, and 30 nmol/kg, so that the estimated BP_{ND} would be high, intermediate, and low within the range in which the linear correlation held. The injection interval was set to 50 mins, because it has been reported in monkey studies that 50 mins scan duration could provide reliable BP_{ND} estimates even for TACs with high and low BP_{ND} values (Ikoma *et al*, 2009). In our present studies on monkeys with this protocol, injected masses increased with each successive injection, but amounts of administered radioactivity remained fairly constant, i.e., 57, 60, and 31 MBq. Therefore, the signal to noise ratio of image quality did not change seriously for each injection.

In the usual graphical analysis by nonsequential multiple PET scans, the molar amount of administered [^{11}C]raclopride for each scan is adjusted by varying the specific activity of administered [^{11}C] raclopride. Several investigators have attempted to perform multiple injections of ligands with PET studies to obtain receptor density and affinity by changing specific activity with a detailed model equation (Delforge *et al*, 1995; Millet *et al*, 1995; Morris *et al*, 1996; Muzic *et al*, 1996; Christian *et al*, 2004; Gallezot *et al*, 2008). Meanwhile, our approach requires only one synthesis of [^{11}C]raclopride, which is split to three with different mass of raclopride with same specific activity. By keeping the specific activity throughout scan, we can directly interpret PET counts in pmol/mL unit.

In the simulations of B_{max} and K_d estimation with this single PET scan approach, B_{max} and K_d were overestimated compared with the true values, just as seen in the three PET scan approach. Furthermore, estimates of both parameters were higher than those in the three PET scan approach. In the single PET scan approach, the error because of assumptions of the reference tissue approach could be more severe than for the three PET scan approach, because the residual radioactivities at the times of the second and third injections could propagate to error of B^{ref} or BP_{ND} estimates. This was shown to be the case in the simulation study, in which the relationship between the BP_{ND} and B^{ref} in the third injection was a little different from that in the first injection (Figure 2). Furthermore, our approach assumes that BP_{ND} is promptly altered by the next injection, but this is in fact not exactly the case. We showed the bias of the estimated BP_{ND} related to this assumption (Ikoma *et al*, 2009), and the estimated B_{max} and K_d in this paper consequently could be biased. However, in the

simulations, B_{max} and K_d estimated by the MI-GA changed according to the variation of the true values (Figure 3), demonstrating this approach could be applied to the quantitative evaluation of B_{max} and K_d from a single session of PET scanning.

Monkey Studies

In the simulations, we demonstrated that the MI-GA could detect density and affinity of dopamine D_2 receptors. Furthermore, we demonstrated the validity of the proposed method using actual data from monkeys. As a result, the three BP_{ND} data points calculated from the single PET scan with three sequential injections of different administration masses were almost on a straight line, and estimated values of B_{max} and K_d were very close to those previously obtained *in vitro* ($B_{max}=25.7$ pmol/g) (Madras *et al*, 1988) or *in vivo* by the conventional method in monkeys ($B_{max}=22$ pmol/mL, $K_d=13.5$ nmol/L) (Doudet *et al*, 2003). The estimates by the single PET scan approach were slightly higher than those by the three PET scan approach, and this was consistent with the results from the current simulations.

Although we investigated only three monkeys in this study, the values of B_{max} in the partially denervated striata was higher than in normal striatum, whereas the apparent affinity was unaffected by the MPTP lesions. Likewise Rinne *et al* (1995) reported a 35% increase in the D_2 B_{max} in the putamen contralateral to the side of predominant motor symptoms, without any discernible effect on apparent affinity. In our monkey measurements, in the hemilesioned monkey, the B_{max} was elevated by 31% on the denervated side. In the animal with bilateral MPTP lesion, the B_{max} in both striata was higher than in the normal animal, or in the unlesioned side of the hemiparkinsonian animal, despite no significant changes in K_d values: the results were consistent with those of the previous report.

In addition to the results of ROI analysis, which disclosed bulk D_2 receptor characteristics in the whole striatum, parametric imaging of B_{max} and K_d (as shown in Figure 5) suggested a potential significance in regional estimation of D_2 receptor characteristics. Although ROI analysis disclosed higher B_{max} values in the MPTP-infused side of the striatum, the parametric imaging showed the increase of B_{max} was more evident in the dorsal and posterior parts of the striatum. A similar finding of preferential lesion in dorsal and posterior parts of the striatum has been reported based on neurochemical and pathological assessments of MPTP-lesioned monkeys (Oiwa *et al*, 2003). As the current parametric imaging may have significant artifacts, such as those arising from low signal-to-noise ratio, partial volume effects, small number of points, the situation should be improved through the use of a higher resolution PET scanner.

Potential Limitations of the Multiple-Injection Graphical Analysis

The multiple-injection approach is able to assess the B_{max} and K_d for receptor studies in a single PET scan with single radiosynthesis, and shortened study period as compared with a conventional approach. This approach might also be applicable to other PET ligands and receptor types, but with several caveats: First, it is necessary to evaluate whether the reference region can be used as the free TAC of the target region. The kinetics of the target and reference regions is affected by the value of each rate constant, i.e., K_1, k_2, B_{max}, and K_d, that differ between species and radioligands. The difference between C_{ref} and C_f often causes an error in B^{ref}, and the estimated B_{max} and K_d should be interpreted with caution when the reference region has considerably different kinetics. Second, the molar amounts of administered ligand need to be selected such that the resultant BP_{ND} will be within the range in which the linear relationship between BP_{ND} and B holds. In the case of regions with low BP_{ND}, and small extent of the necessary linear relationship, it may be difficult to determine B_{max} and K_d reliably. Third, the interval of three injections should be determined so that the free ligand TAC has a transient equilibrium within the scan duration of each injection, especially when the injected mass is small, i.e., BP_{ND} is high. The radioligand [^{11}C]raclopride dissociates rapidly from the receptors, allowing equilibration of binding to be established *in vivo* within the time span of PET experiments (Farde *et al*, 1989; Ito *et al*, 1998). However, those ligands with slow kinetics, such as [^{18}F]fallypride require a longer scan duration such that the present graphical analysis may not be suitable in all instances. Despite these limitations, by optimizing the administered mass and the time interval between three injections of [^{11}C]raclopride, we have shown that the multiple-injection approach can determine B_{max} and K_d values as effectively as an approach using three separate scans, but within a single scan time of 150 mins.

Moreover, the bias of B_{max} and K_d estimated by the single scan approach with two injections was not larger than that by the single scan approach with three injections in the simulations (data not shown), and points of the second and third injections in MI-GA were almost on the same line in the monkey studies (Figure 6). Therefore, there is a possibility of reducing scan time and exposure further using only two injections, though the effect of statistical noise on estimates should be considered.

Conclusion

We developed the method for estimating B_{max} and K_d values in a single session of PET scanning with multiple injections of [^{11}C]raclopride. Our simulations showed that the MI-GA could detect B_{max} and K_d values by using the optimal injection protocol. We

also demonstrated in monkey studies that B_{max} and K_d values estimated by our proposed approach were proper compared with previous monkey studies or our studies by the conventional method. The proposed method made it possible to determine the dopamine D_2 receptor density and affinity by a 150 mins PET scan with three injections of [^{11}C]raclopride at 50 mins intervals.

Acknowledgements

We thank Dr Jun Takahashi (Kyoto University) for providing us animals for this study. This research was supported by the Ministry of Education, Culture, Sports, Science and Technology of Japan (MEXT) grant-in-aid for Young Scientists (B) (No. 20790839), grant-in-aid for Scientific Research (C) (No. 09019855) (TH), Kobe Cluster I and II, and the Ministry of Health, Labour, and Welfare of Japan (MHLW) Health Science Research Grant, H17-025 (TH, HI). We are grateful to members of Department of Investigative Radiology, National Cardiovascular Center Research Institute, for their support of PET experiment and for helpful suggestions.

Conflict of interest

The authors declare no conflict of interest.

References

Bankiewicz KS, Oldfield EH, Chiueh CC, Doppman JL, Jacobowitz DM, Kopin IJ (1986) Hemiparkinsonism in monkeys after unilateral internal carotid artery infusion of 1-methyl-4-phenyl-1,2,3,6-tetrahydropyridine (MPTP). *Life Sci* 39:7–16

Christian BT, Narayanan T, Shi B, Morris ED, Mantil J, Mukherjee J (2004) Measuring the *in vivo* binding parameters of [^{18}F]-fallypride in monkeys using a PET multiple-injection protocol. *J Cereb Blood Flow Metab* 24:309–22

Cross AJ, Crow TJ, Owen F (1981) ^{3}H-Flupenthixol binding in post-mortem brains of schizophrenics: evidence for a selective increase in dopamine D2 receptors. *Psychopharmacology (Berl)* 74:122–4

Delforge J, Pappata S, Millet P, Samson Y, Bendriem B, Jobert A, Crouzel C, Syrota A (1995) Quantification of benzodiazepine receptors in human brain using PET, [^{11}C]flumazenil, and a single-experiment protocol. *J Cereb Blood Flow Metab* 15:284–300

Doudet DJ, Holden JE (2003) Sequential versus non-sequential measurement of density and affinity of dopamine D_2 receptors with [^{11}C]raclopride: Effect of methamphetamine. *J Cereb Blood Flow Metab* 23:1489–94

Doudet DJ, Jivan S, Holden JE (2003) *In vivo* measurement of receptor density and affinity: comparison of the routine sequential method with a nonsequential method in studies of dopamine D_2 receptors with [^{11}C]raclopride. *J Cereb Blood Flow Metab* 23:280–4

Farde L, Ehrin E, Eriksson L, Greitz T, Hall H, Hedström CG, Litton JE, Sedvall G (1985) Substituted benzamides as ligands for visualization of dopamine receptor binding in the human brain by positron emission tomography. *Proc Natl Acad Sci USA* 82:3863–7

Farde L, Eriksson L, Blomquist G, Halldin C (1989) Kinetic analysis of central [^{11}C]raclopride binding to D_2-dopamine receptors studied by PET — A comparison to equilibrium analysis. *J Cereb Blood Flow Metab* 9: 696–708

Farde L, Hall H, Ehrin E, Sedvall G (1986) Quantitative analysis of D_2 dopamine receptor binding in the living human brain by PET. *Science* 231:258–61

Farde L, Wiesel FA, Hall H, Halldin C, Stone-Elander S, Sedvall G (1987) No D_2 receptor increase in PET study of schizophrenia. *Arch Gen Psychiatry* 44:671–2

Farde L, Wiesel FA, Stone-Elander S, Halldin C, Nordström AL, Hall H, Sedvall G (1990) D_2 dopamine receptors in neuroleptic-naive schizophrenic patients. A positron emission tomography study with [^{11}C]raclopride. *Arch Gen Psychiatry* 47:213–9

Gallezot JD, Bottlaender MA, Delforge J, Valette H, Saba W, Dollé F, Coulon CM, Ottaviani MP, Hinnen F, Syrota A, Grégoire MC (2008) Quantification of cerebral nicotinic acetylcholine receptors by PET using 2-[^{18}F]fluoro-A-85380 and the multiinjection approach. *J Cereb Blood Flow Metab* 28:172–89

Gunn RN, Lammertsma AA, Hume SP, Cunningham VJ (1997) Parametric imaging of ligand-receptor binding in PET using a simplified reference region model. *Neuroimage* 6:279–87

Guttman M, Seeman P (1985) L-dopa reverses the elevated density of D_2 dopamine receptors in Parkinson's diseased striatum. *J Neural Transm* 64:93–103

Hall H, Köhler C, Gawell L, Farde L, Sedvall G (1988) Raclopride, a new selective ligand for the dopamine-D_2 receptors. *Prog Neuropsychopharmacol Biol Psychiatry* 12:559–68

Herzog H, Tellmann L, Hocke C, Pietrzyk U, Casey ME, Kuwert T (2004) NEMA NU2-2001 guided performance evaluation of four Siemens ECAT PET scanners. *IEEE Trans Nucl Science* 51:2662–9

Ikoma Y, Watabe H, Hayashi T, Miyake Y, Teramoto N, Minato K, Iida H (2009) Quantitative evaluation of changes in binding potential with a simplified reference tissue model and multiple injections of [^{11}C]raclopride. *Neuroimage* 47:1639–48

Ito H, Hietala J, Blomqvist G, Halldin C, Farde L (1998) Comparison of the transient equilibrium and continuous infusion method for quantitative PET analysis of [^{11}C]raclopride binding. *J Cereb Blood Flow Metab* 18:941–50

Joyce JN, Lexow N, Bird E, Winokur A (1988) Organization of dopamine D_1 and D_2 receptors in human striatum: receptor autoradiographic studies in Huntington's disease and schizophrenia. *Synapse* 2:546–57

Köhler C, Hall H, Ogren SO, Gawell L (1985) Specific *in vitro* and *in vivo* binding of ^{3}H-raclopride. A potent substituted benzamide drug with high affinity for dopamine D-2 receptors in the rat brain. *Biochem Pharmacol* 34:2251–9

Lammertsma AA, Hume SP (1996) Simplified reference tissue model for PET receptor studies. *Neuroimage* 4:153–8

Logan J, Fowler JS, Volkow ND, Wang GJ, Ding YS, Alexoff DL (1996) Distribution volume ratios without blood sampling from graphical analysis of PET data. *J Cereb Blood Flow Metab* 16:834–40

Logan J, Volkow ND, Fowler JS, Wang GJ, Fischman MW, Foltin RW, Abumard NN, Vitkun S, Gatley SJ, Pappas N, Hitzemann R, Shea CE (1997) Concentration and occupancy of dopamine transporters in cocaine abusers with [^{11}C]cocaine and PET. *Synapse* 27:347–56

Madras BK, Fahey MA, Canfield DR, Spealman RD (1988) D1 and D2 dopamine receptors in caudate-putamen of nonhuman primates (*macaca fascicularis*). *J Neurochem* 51:934–43

Millet P, Delforge J, Mauguiere F, Pappata S, Cinotti L, Frouin V, Samson Y, Bendriem B, Syrota A (1995) Parameter and index images of benzodiazepine receptor concentration in the brain. *J Nucl Med* 36:1462–71

Mintun MA, Raichle ME, Kilbourn MR, Wooten GF, Welch MJ (1984) A Quantitative model for the *in vivo* assessment of drug binding sites with positron emission tomography. *Ann Neurol* 15:217–27

Morris ED, Babich JW, Alpert NM, Bonab AA, Livni E, Weise S, Hsu H, Christian BT, Madras BK, Fischman AJ (1996) Quantification of dopamine transporter density in monkeys by dynamic PET imaging of multiple injections of ^{11}C-CFT. *Synapse* 24:262–72

Muzic RR, Nelson AD, Saidel GM, Miraldi F (1996) Optimal experiment design for PET quantification of receptor concentration. *IEEE Trans Med Imaging* 15:2–12

Oiwa Y, Eberling JL, Nagy D, Pivirotto P, Emborg ME, Bankiewicz KS (2003) Overlesioned hemiparkinsonian non human primate model: correlation between clinical, neurochemical and histochemical changes. *Front Biosci* 8:155–66

Rinne JO, Laihinen A, Ruottinen H, Ruotsalainen U, Någren K, Lehikoinen P, Oikonen V, Rinne UK (1995) Increased density of dopamine D_2 receptors in the putamen, but not in the caudate nucleus in early Parkinson's disease: a PET study with [^{11}C]raclopride. *J Neurol Sci* 132:156–61

Scatchard G (1949) The attractions of proteins for small molecules and ions. *Ann NY Acad Sci* 51:660–72

Seeman P, Bzowej NH, Guan HC, Bergeron C, Reynolds GP, Bird ED, Riederer P, Jellinger K, Tourtellotte WW (1987) Human brain D_1 and D_2 dopamine receptors in schizophrenia, Alzheimer's, Parkinson's, and Huntington's diseases. *Neuropsychopharmacology* 1:5–15

Takagi Y, Takahashi J, Saiki H, Morizane A, Hayashi T, Kishi Y, Fukuda H, Okamoto Y, Koyanagi M, Ideguchi M, Hayashi H, Imazato T, Kawasaki H, Suemori H, Omachi S, Iida H, Itoh N, Nakatsuji N, Sasai Y, Hashimoto N (2005) Dopaminergic neurons generated from monkey embryonic stem cells function in a Parkinson primate model. *J Clin Invest* 115:102–9

Watabe H, Ohta Y, Teramoto N, Miyake Y, Kurokawa M, Yamamoto A, Ose Y, Hayashi T, Iida H (2006) A novel reference tissue approach for multiple injections of [C-11]Raclopride. *Neuroimage* 31:T73

Wong DF, Wagner Jr HN, Tune LE, Dannals RF, Pearlson GD, Links JM, Tamminga CA, Broussolle EP, Ravert HT, Wilson AA, Toung JK, Malat J, Williams JA, O'Tuama LA, Snyder SH, Kuhar MJ, Gjedde A (1986) Positron emission tomography reveals elevated D_2 dopamine receptors in drug-naive schizophrenics. *Science* 234:1558–63

Appendix

The multiple-injection two-tissue four-parameter compartment model is based on the following differential equations:

$$\frac{dC_f}{dt} = K_1 C_p(t) - (k_2 + k_3) C_f(t) + k_4 C_b(t) \qquad \text{(A1)}$$

$$\frac{dC_b}{dt} = k_3 C_f(t) - k_4 C_b(t) \qquad \text{(A2)}$$

where C_p is the radioactivity concentration of metabolite-corrected plasma, C_f and C_b are the concentrations of radioactivity for free and specifically bound ligand in tissue, respectively.

Equations (A1) and (A2) are solved with the radioactivity concentration of C_f and C_b at the time of injection, that is $C_f(0)$ and $C_b(0)$, then $C_f(t)$, $C_b(t)$ and total radioactivity concentration in tissue $C_t(t)$ are expressed as following equations:

$$\begin{aligned} C_f(t) = & \frac{K_1}{\alpha_2 - \alpha_1}\{(k_4 - \alpha_1)e^{-\alpha_1 t} - (k_4 - \alpha_2)e^{-\alpha_2 t}\} \otimes C_p(t) \\ & + \frac{1}{\alpha_2 - \alpha_1}\{(k_4 - \alpha_1)C_f(0) + k_4 C_b(0)\}e^{-\alpha_1 t} \\ & - \frac{1}{\alpha_2 - \alpha_1}\{(k_4 - \alpha_2)C_f(0) + k_4 C_b(0)\}e^{-\alpha_2 t} \end{aligned} \qquad \text{(A3)}$$

$$\begin{aligned} C_b(t) = & \frac{K_1 k_3}{\alpha_2 - \alpha_1}\left(e^{-\alpha_1 t} - e^{-\alpha_2 t}\right) \\ & \otimes C_p(t) + \frac{k_3}{\alpha_2 - \alpha_1}\left(C_f(0) + \frac{k_4}{k_4 - \alpha_1} C_b(0)\right)e^{-\alpha_1 t} \\ & - \frac{k_3}{\alpha_2 - \alpha_1}\left(C_f(0) + \frac{k_4}{k_4 - \alpha_2} C_b(0)\right)e^{-\alpha_2 t} \\ & + \left(\frac{k_3 k_4}{(k_4 - \alpha_1)(k_4 - \alpha_2)} + 1\right) C_b(0) e^{-k_4 t} \end{aligned} \qquad \text{(A4)}$$

$$\begin{aligned} C_t(t) = & \frac{K_1}{\alpha_2 - \alpha_1}\{(k_3 + k_4 - \alpha_1)e^{-\alpha_1 t} - (k_3 + k_4 - \alpha_2)e^{-\alpha_2 t}\} \\ & \otimes C_p(t) + \frac{k_3 + k_4 - \alpha_1}{\alpha_2 - \alpha_1}\left(C_f(0) + \frac{k_4}{k_4 - \alpha_1} C_b(0)\right)e^{-\alpha_1 t} \\ & - \frac{k_3 + k_4 - \alpha_2}{\alpha_2 - \alpha_1}\left(C_f(0) + \frac{k_4}{k_4 - \alpha_2} C_b(0)\right)e^{-\alpha_2 t} \\ & + \left(\frac{k_3 k_4}{(k_4 - \alpha_1)(k_4 - \alpha_2)} + 1\right) C_b(0) e^{-k_4 t} \\ \alpha_{1,2} = & \frac{(k_2 + k_3 + k_4) \mp \sqrt{(k_2 + k_3 + k_4)^2 - 4k_2 k_4}}{2} \end{aligned} \qquad \text{(A5)}$$

Circ J 2009; **Suppl A:** A-55–A-60

Heart Transplantation

Takeshi Nakatani, MD

A total of 59 heart transplantations (HTx) have been performed in Japan as of September, 2008, since the Organ Transplantation Law was settled in October 1997. The majority of recipients were suffered from dilated cardiomyopathy and waiting condition of all recipients were status 1. The mean waiting time was 777 day; 50 patients (85%) were supported by several types of left ventricular assist systems (LVAS) and the mean duration of support was 780 days. The majority of patients underwent operation by modified bicaval method with Celsior solution for cardiac preservation, and 64% of recipients were administered triple therapy with cyclosporine, mycophenolate mofetil, and steroid as the initial immunosuppressive regimen. The 9-year survival rate was 94%, which was superior to that of the international registry. HTx in Japan has been very limited by a severe shortage of donors, but the results have been excellent even though the majority of recipients were waiting for long-term with a LVAS as a bridge to HTx. (*Circ J* 2009; **Suppl A:** A-55–A-60)

Key Words: Bridge to heart transplantation; Heart transplantation; Left ventricular assist systems

The first human-to-human heart transplantation (HTx) was performed in South Africa on December 3, 1967[1] and by the end of 1968, 102 HTx had been performed in 52 institutions. However, the results were disappointing, with 60% early mortality and a mean survival of only 29 days[2] During the 1970s, a few institutions continued to perform HTx. The transvenous endomyocardial biopsy technique with a histologic system of grading was developed for monitoring heart allograft rejection[3] and in the early 1980s, the introduction of cyclosporine for immunosuppression improved the results of HTx. Following this progress, the number of HTx procedures increased dramatically and it has become the standard option for end-stage heart failure. According to the international registry, more than 80,000 HTx have been performed worldwide to date[4]

In Japan, the Organ Transplantation Law was settled in October 1997, and first HTx under this law was performed in 1999. Since then, a total of 59 HTx have been performed in Japan as of September 2008. From May 2001, HTx for dilated cardiomyopathy (DCM) and the dilated phase of hypertrophic cardiomyopathy (dHCM) was approved as highly advanced medical technology. Enforcement of HTx performed in institutes selected by the Joint Committee of Transplant-related Societies was covered by health insurance from April 2006.

Listing and Waiting for HTx

HTx is considered a therapeutic option for the patient with advanced heart disease that is life-threatening and refractory to the traditional medical and/or surgical therapies. Major heart diseases are DCM, dHCM and ischemic heart disease (IHD). Of those, DCM and dHCM should be diagnosed by endomyocardial biopsy.

If patients fulfill the following conditions, they are candidates for HTx.

1. Require prolonged or repeated hospitalization.
2. Continuing to be New York Heart Association class 3–4 despite traditional therapy including β-blockers and angiotensin-converting enzyme inhibitors.
3. Life-threatening severe arrhythmia that is uncontrollable with traditional antiarrhythmic treatment.
4. Under 60 years of age (desirable).

The following conditions render them unsuitable.

1. Severe non-cardiac disease (eg, severe dysfunction of liver or kidney, significant obstructive pulmonary disease, malignancy, severe autoimmune disease, collagen disease, etc).
2. Active peptic ulcer or infection, severe diabetes mellitus, excessive obesity.
3. Tobacco, alcohol or drug abuse.
4. Psychoneurosis.
5. Fixed pulmonary vascular resistance greater than 6 Wood units.
6. HIV antibody positive.

In the investigation of HTx candidacy, a therapeutic approach excepting HTx, predicted life expectancy, and compliance with post-transplant treatment should be considered carefully because medical therapy including immunosuppression is necessary throughout the patient's lifetime. In Japan, determination of HTx candidates has 2 phases. Heart transplant committees of the Japanese Circulation Society as well as each institution examine the HTx indications. When the patient is accepted as a HTx candidate by both committees, informed consent of the candidate and family is obtained at each HTx institution. After that, the candidate is enrolled in the Japan Organ Transplant Network (JOTNW). HTx operations are now limited to 6 institutes chosen by the Joint Committee of Transplant-related Societies.

Treatment for heart failure continues while waiting for HTx. In some cases, native heart function will recover enough to quit the waiting list. In other cases, candidacy will be lost because of severe organ dysfunction, infection or various disorders. Therefore, review of candidacy is performed every 6 months. When heart failure progresses and

(Received May 13, 2009; accepted May 15, 2009; released online June 5, 2009)

Department of Organ Transplantation, National Cardiovascular Center, Suita, Japan
Mailing address: Takeshi Nakatani, MD, Department of Organ Transplantation, National Cardiovascular Center, 5-7-1 Fujishiro-dai, Suita 565-8565, Japan. E-mail: tnakatan@hsp.ncvc.go.jp

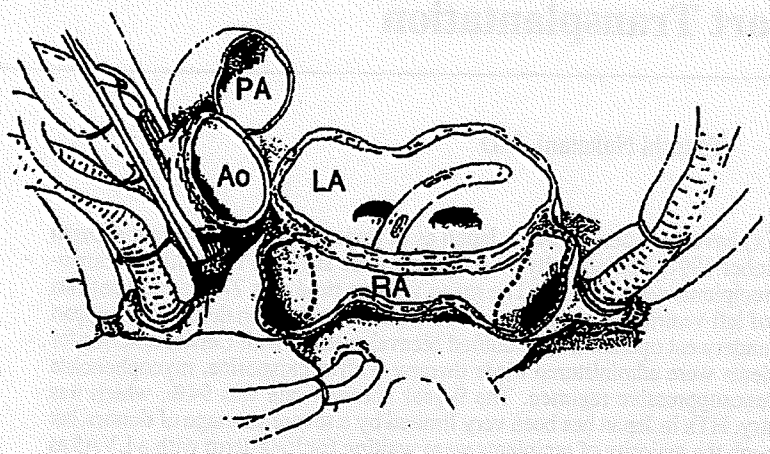

Figure 1. Modified bicaval method[5] PA, pulmonary artery; Ao, aorta; LA, left atrium; RA, right atrium.

organ function deteriorates, application of a ventricular assist system (VAS) will be considered as a bridge-to-transplantation. At present, the Toyobo-National Cardiovascular Center type VAS is used under health insurance. Several types of implantable left VAS (LVAS) are applied as clinical trials. Many listed cases are supported with a VAS before listing or while waiting for HTx in Japan.

Examination of Donor Heart and Selection of Candidate for HTx

First, the appropriateness of the donor for organ transplantation is reviewed. If there is active systemic infection, positivity for HIV antibody, HTLV-1 antibody, hepatic B surface antigen or HCV antibody, diagnosis or suspicion of Creutzfeld-Jakob disease, or malignant tumor, the donor is unsuitable. Subsequently, examination as a donor for HTx is performed. If there is diagnosed heart disease, cardiac trauma or a history of open-heart surgery, the donor is unsuitable. As a donor for HTx, age less than 60 years is desirable; in men over 45 years old or women over 50 years old, consideration must be given to coronary arteriosclerosis. Cardiac condition should be carefully examined by electrocardiography and echocardiography, especially when large doses of inotropic agents have been used (>10μg·kg^{-1}·min^{-1} of dopamine equivalency). Final judgment is confirmed by visual inspection and palpation of the donor heart.

A candidate for recipient is chosen from the waiting list of the JOTNW when the potential donor is considered suitable. Selection from the list is according to the following policy: matching blood type (identical/compatible), size (body weight between 80% and 130% of the donor is suitable), and negative in direct cross-match. When several candidates are selected, the maximum period of donor heart ischemia before operation within 4 h, status of waiting (priority to status 1 candidates), and the waiting time. As status 1, consideration is given to (1) supported by VAS, (2) supported by IABP, (3) under ventilator support, and (4) continuous infusion of inotropes treated in the intensive care rooms such as ICU or CCU.

Transplant Operation

One of the key issues in HTx is donor selection and management of the donor. The ideal cardiac donor is of a suitable age with stable hemodynamics. Management to stabilize hemodynamics is important for expanding the donor pool. Cause of death, cardiac arrest and cardiopulmonary resuscitation, chest trauma, and medical history, especially cardiovascular disease, are checked. Hemodynamics are usually evaluated by vital signs, 12-lead ECG, transthoracic echocardiography, and administration of drugs such as catecholamine. Many donors show echocardiographic abnormalities and/or significant pressor/inotrope requirement. Abnormalities of the coronary arteries is usually checked under direct vision and the final decision of acceptance is made by the donor team.

Because no one can predict of the timing of donation, the transplant team must always be available in a short time. Furthermore, proximity of the donor and recipient teams is important because the permissible ischemic time for the heart is shorter than that for other organs.

Donor Operation

The final assessment of the donor heart is performed by visual inspection and palpation to check for contusion, recent ischemic events, heart disease and contractility after median sternotomy. Subsequently, the ascending aorta, pulmonary artery (PA), and superior and inferior venae cava (SVC, IVC) are dissected and preparation for cannulation for cardioplegia is performed in the ascending aorta. The donor heart team waits while the preparations are done by the other organ recovery teams. After completion of dissection of additional organs, heparin is given and the cardioplegia line is inserted into the ascending aorta and the cardioplegic solution is flushed. When the lungs are harvested at the same time, cannulation for pulmonary preservation is performed in the main PA by the pulmonary *donor team.* The SVC is tied and cut after infusion of pulmonary preservation solution from the PA. Subsequently, the ascending aorta is cross-clamped and pressurized cardioplegic solution is infused with cutting of the IVC.

In the bicaval method of recipient operation, the length of both the SVC and IVC is important. The site in the IVC is near the right atrium when the liver is harvested at the same time. The pulmonary vein and left atrium region are isolated with the pulmonary donor team. The SVC is cut right under the azygos vein and the ascending aorta is cut as long as possible. The PA is cut at the bifurcation and then the heart is excised, wrapped three times in plastic bags containing cardioplegic solution and transported within an

icebox. Various types of cardioplegic solution can be used. We used St Thomas solution of the extracellular fluid type at first, but changed to Celsior solution from the 7th case.

Recipient Operation

In the standard technique for HTx developed by Lower-Shumway, the left atrial anastomosis is performed first and then the right atrial anastomosis after creation of a right atrial cuff, which is created by an incision from the orifice of the IVC toward the right atrial appendage.[5] In the bicaval method, the recipient right atrium is excised by transecting the SVC and the junction between the right atrium and IVC. The donor atria are preserved and left atrial anastomosis with a separate bicaval anastomosis is performed. The bicaval method has been modified to leave a strip of the posterior right atrial wall as a bridge connecting both venae cava by Kitamura et al.[6] In this method, the bridging posterior right atrium serves as a landmark of the right atrial cuff distorted by the caval snares. Adjustment of the length between the SVC and IVC is easy for a small donor heart because of the absence of shrinkage and retraction of the divided atrial cuffs (**Figure 1**).

A median sternotomy is performed. In patients with LVAS implantation, dissection of the heart must be done carefully because of severe adhesion, especially around the inlet and outlet cannulae including LV apex. The femoral vessels are prepared for emergency cannulation. Before the arrival of the donor heart, the recipient's heart and great vessels are exposed and prepared for cannulation. The recipient is heparinized and cannulation for cardiopulmonary bypass is performed. The site of aortic cannulation is distal to the anastomosis of the outlet cannula of the LVAS. For venous cannulation, right-angled cannulae are preferable because they do not obstruct the suturing of the bicaval anastomoses.

When the donor heart has arrived in the operating room, recipient heart excision is started with aortic cross-clamping and snaring of the SVC and IVC. An incision is made in the right atrium and extended to the coronary sinus. The aorta is divided just above the aortic valve and then the PA is divided just distal to the pulmonary valve. The left atrium is divided, starting at the septum and extending across the dome to the base of the left atrial appendage. The incision is continued to the mitral valve. Then the heart is removed. When a LVAS has been implanted, care must be taken to remove the anastomosis site of the outflow cannula in the ascending aorta. The inflow cannula is detached from the LV apex.

The donor heart is inspected for abnormalities, such as a patent foramen ovale (PFO), and valvular anomalies. If a PFO is found, it is closed from the right atrial side. The PA and aorta are separated. Next, the pulmonary vein openings are connected, creating a large left atrial cuff. In the Lower-Shumway method, the SVC is doubly ligated and the right atrium is opened from the IVC to the right atrial appendage without injuring the sinus node.

For the recipient anastomoses, the left atrial anastomosis is performed first. The donor left atrial cuff is sutured to the recipient's left atrium using a long 4-0 prolene suture from the level of the left superior pulmonary vein. A venting catheter is inserted in the left ventricle through the right pulmonary vein via the mitral valve. After completion of the left atrial anastomosis, the subsequent anastomoses are performed according to the ischemic time. Usually, the pulmonary anastomosis is performed after trimming to avoid excess length and possible kinking. This anastomosis is performed end-to-end with a running 5-0 prolene suture. Then the donor and recipient aortas are anastomosed end-to-end with a running 4-0 prolene suture. The donor IVC is anastomosed to the recipient IVC–atrial cuff using a 5-0 prolene suture. After that, terminal cardioplegic solution is infused and the aortic cross-clamp is removed. The donor SVC and recipient SVC–atrial cuff are anastomosed using a 5-0 prolene suture.

Usually inotropic support such as dobutamine is given and the patient is weaned from cardiopulmonary bypass after confirming air removal and ventricular function by transesophageal echocardiography. Heart rate control is needed because the donor heart is denervated and a heart rate of 90–120 beats/min is maintained by infusion of isoproterenol or temporary pacing. Immunosuppression during the operation is performed by infusing 500 mg of methylprednisolone twice: at the beginning of operation and just before declamping of the aorta.

In the case of LVAS implantation, the blood pump and cannulae are removed.

Intensive Care After HTx

The hemodynamic problems of transplant patients in the intensive care unit (ICU) at National Cardiovascular Center are summarized as denervated heart, transient cardiac dysfunction, pulmonary hypertension, and donor–recipient size mismatch.[7] Cardiac pacing is applied to all patients and isoproterenol infusion is required in some cases to maintain an appropriate heart rate. Infusion of low-dose dopamine and atrial natriuretic peptide is performed for preservation of cardiac and renal function. Acute renal insufficiency occurred in 1 patient, who needed transient continuous hemodiafiltration. Early removal of catheter and tubes was attempted to reduce the risk of infection. In 1 case of donor–recipient size mismatch, cardiogenic pulmonary edema developed immediately after tracheal extubation, probably because of wound pain and afterload mismatch. Management of the denervated heart and preservation of renal function, in addition to conventional intensive care, are important in the intensive care of HTx patients.

Management After HTx

Important factors influencing the prognosis of HTx patients are primary graft failure, acute rejection, transplant coronary artery disease, infection, and malignancy.

Primary Graft Failure

Donor heart function, the preservation method, and the surgical method of harvesting affect graft function. If the donor has been infused with high doses of inotropic agents or has had an episode of cardiac arrest, donor heart function should be investigated carefully by electrocardiography and echocardiography. It is important to shorten the ischemic time of the donor heart as much as possible to preserve its function. As for cardioplegia, Celsior solution is easily available at donor hospitals. Transportation is another factor in shortening the ischemic time. Use of private jets or helicopter under direction of the JOTNW is desirable to ensure close communication between the donor and recipient teams.

Acute Rejection

Control of acute rejection is important and the results of

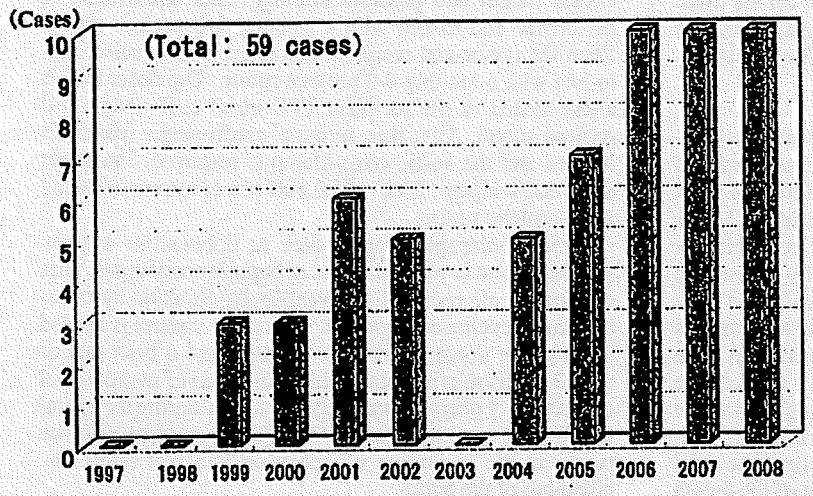

Figure 2. Year distribution of heart transplantation in Japan![3]

HTx have improved after adoption of a new immunosuppressive drug, cyclosporine, and development of the endomyocardial biopsy method from an internal jugular vein as the diagnostic procedure. Acute rejection is frequent within the first year and there are many asymptomatic cases. Therefore, scheduled endomyocardial biopsy is performed and the histopathologic judgment is based on the International Society for Heart and Lung Transplantation (ISHLT) standardized cardiac biopsy grading[8]

For immunosuppressive therapy, a 3-drug regimen including a calcineurin inhibitor (cyclosporine (Neoral®) or tacrolimus (Prograph®)) in combination with an antimetabolite (mycophenolate mofetil (Cellcept®) or azathioprine) and steroid (predonine) is generally used[4] Induction therapy with monoclonal or polyclonal antibodies was also used in several cases. We have used, murine monoclonal CD3 antibody (OKT3®) or IL-2 monoclonal antibody (basiliximab) in cases of severe renal dysfunction in the perioperative period.

The immunosuppressive agents are controlled by pharmacokinetic parameters, including trough level and the area under the plasma concentration curve[9,10] ISHLT grade 3A or higher rejection is usually treated with steroid pulse therapy. If there is resistance to pulse therapy, cytolytic therapy consisting of monoclonal or polyclonal antibodies is instituted. Humoral or antibody-mediated rejection will occur if there is attacking of donor-specific antibodies![1] The panel reactive antibody test is useful for monitoring this, and plasmapheresis, intravenous immunoglobulin (IVIg), and rituximab (anti-B-cell antibodies) are used to treat humoral rejection.

Transplant Coronary Artery Disease (TxCAD)

TxCAD is thought to be chronic rejection of the allograft with the immunologic attack directed against the vascular endothelium of the allograft. Histologically, the intimal lesions are concentric, diffuse and extensive. Several factors, such as activation of T lymphocytes, antibodies, acute rejection, and cytomegalovirus (CMV) infection, are considered as possible etiologies, but the precise mechanism of TxCAD is still unclear.

Cardiogenic shock or sudden death from arrhythmia develops without chest pain because of denervation of the transplanted heart. We monitored TxCAD by routine coronary arteriography and intravascular ultrasonography at biopsy 3 months after transplant and at the annual checkup. Coronary artery bypass grafting, percutaneous transluminal coronary angioplasty or stenting are only palliative because of the diffuse nature of TxCAD. Recently, the proliferation signal inhibitors or mammalian target-of-rapamycin inhibitors, everolimus and sirolimus, demonstrated a benefit in reducing maximal intimal thickness and subsequently TxCAD in de novo HTx recipients![2] Everolimus was introduced to Japan in 2007, and is used for patients with TxCAD. Long-term follow-up of these patients is essential.

Infection

Infection is the leading cause of death of HTx recipients during the 1st year after transplant, according to the ISHLT registry[4] Bacterial infection is common during the 1st month after transplant and subsequently, opportunistic infections, such as CMV and herpes simplex virus, increase. CMV infection is considered to be a risk factor of TxCAD, so at the National Cardiovascular Center, CMV-PCR is performed routinely. In the management of infection, care should be taken to prevent it and to treat it early.

Malignancy

Malignancy, including lymphoma, is the cause of death in over 20% of HTx recipients who survive more than 3 years from JSHLT registry[4] Lymphoma (post-transplant lymphoproliferative disorder: PTLD) is a common tumor after transplantation and it is speculated that it might be related to the overall level of immunosuppression, especially the calcineurin inhibitor. Epstein-Barr virus (EBV) has a possible causative role in PTLD, so we perform check of EVB-PCR at routine follow-up visits.

Long-Term Follow-up After HTx

Consideration must be given to hypertension, renal dysfunction, hyperlipidemia, diabetes mellitus to maintain the quality of life of HTx recipients. Adjustment of immunosuppressive drugs is important to reduce side-effects, and early detection of infection, malignancy, and TxCAD improves prognosis.

Results Worldwide

According to the ISHLT registry of 2008[4] over 80,000 HTx have been performed worldwide. Between January

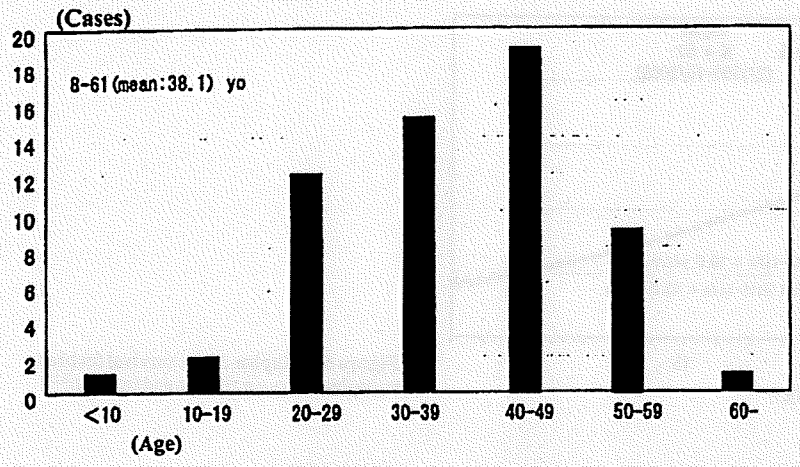

Figure 3. Age distribution of heart transplant recipients in Japan![3]

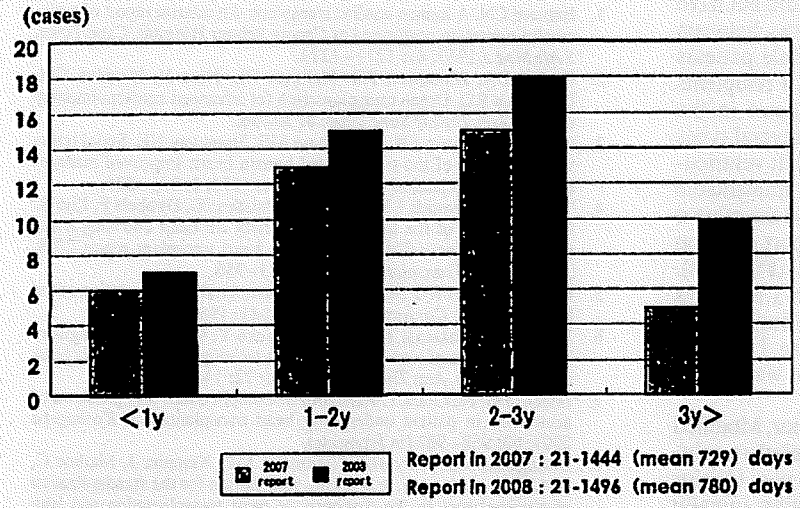

Figure 4. Duration of support with a left ventricular assist system in heart transplant patients in Japan![3]

1982 and June 2006, 74,267 HTx were performed and survival rates were 81.6% at 1 year, 68.6% at 5 years, 50.6% at 10 years, and 19.6% at 20 years. Recent survival rates have improved compared with the early phase of the registry (at 5 years (1982–1991): 64.6%; 70.0%, 1992–2001; 72.3%, 2002–2006). Survival decreases at a linear rate of approximately 3.5% per year. For immunosuppressive therapy, the combination of cyclosporine (or tacrolimus), mycophenolate mofetil, and predonine is the most common, although recently, tacrolimus has overtaken cyclosporine as the most common calcineurin inhibitor. Sirolimus is used in over 10% of recipients at 1-year post transplant. As an induction therapy, use of interleukin-2 receptor antagonist is increasing. According to the functional status reported on the 1-, 3-, 5- and 7-year annual follow-up (between 1995 and June 2006), approximately 90% of survived recipients have no activity limitations up to 7 years after transplant.

Results in Japan

Among the 333 candidates for HTx registered with the JOTNW from October 1997 to September 2008, 59 HTx were performed in 7 institutes (National Cardiovascular Center: 24; Osaka University: 17; Tokyo University: 6; Tokyo Women's Medical University: 4; Saitama Medical

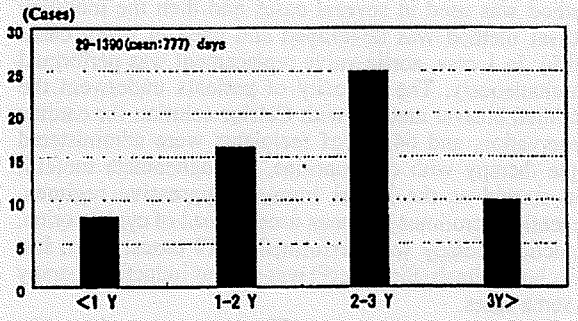

Figure 5. Waiting period for heart transplantation in Japan![3]

University: 3; Kyusyu University: 3; Tohoku University: 2)[13] (Figure 2). Of these cases, the first was performed at Osaka University[14] and subsequently 2 cases were performed at the National Cardiovascular Center in 1999![15] However, 35 candidates underwent HTx abroad and 109 died while on the waiting list; 118 candidates are awaiting HTx and of those, 51% are status 1, 42% are status 2, and 7% are status 3. The main characteristic of the transplanted patients was DCM as the major primary indication for HTx, and IHD was present in 3 of the 59 (5%). In the ISHLT registry, IHD

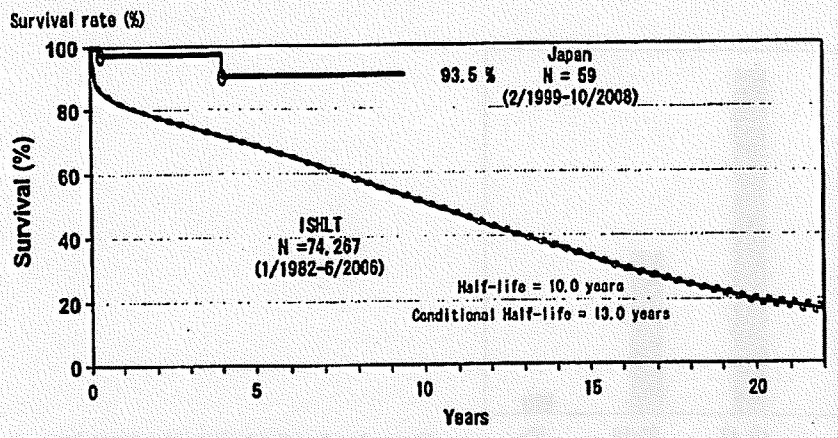

Figure 6. Kaplan-Meier survival for heart transplantation worldwide and in Japan.[3,13]

is the indication in approximately 30% of recipients. In contrast, over 90% of the Japanese HTx recipients did not have IHD. The age distribution of the recipients was between 8 and 61 (mean 38.1) years old (**Figure 3**). Male patients comprised 35 cases and females 17 cases. All recipients were status 1, including 9 with inotropic support in the ICU/CCU. The other 50 patients (84.7%) had several types of LVAS: 36 received the Toyobo LVAS (34: left ventricular drainage, 2: left atria drainage), 10 had an implantable pulsatile LVAS (Novacor: 5, HeartMate: 5), and the other 4 had an implantable non-pulsatile LVAS. Support duration was between 21 and 1,496 days (mean 780 days) (**Figure 4**). Waiting period as status 1 was between 29 to 1,390 days (mean 777 days) (**Figure 5**). The waiting time has recently extended; only 8 cases underwent HTx within 1 year of listing on the JOTNW, and 10 cases have been waiting for more than 3 years.

With regard to the cardioplegic solution, Celsior, Modified Collins solution, St Thomas solution, Bredshnieders solution, and UW solution were used initially, but now Celsior solution is mainly used. For the recipient operation, initially the Lower-Shumway method was used, but the bicaval method was used in several cases and then the modified bicaval method was developed and used in many cases (68%). In 1 case, aortic valve replacement was performed simultaneously. The majority of patients underwent the modified bicaval method with Celsior solution for cardiac preservation, and 64.4% of recipients were administered triple therapy with cyclosporine, mycophenolate mofetil, and steroid as the initial immunosuppressive regimen. Recently, tacrolimus has been used instead of cyclosporine. Induction therapy was performed in 19 cases. From last year, basiliximab (Simulect®) was used as induction therapy in some cases.

Only 2 patients died after HTx (pneumonia: 4 months after HTx; infection: 50 months after HTx). The longest survival is up to 10 years after HTx. The 5-year survival rate is 93.5%, which is superior to that of the international registry (**Figure 6**).

Future Prospects

HTx in Japan has been very limited by a severe shortage of donors, but the results have beene excellent even though the majority of recipients had a LVAS as a bridge to HTx. Progress of the HTx program, including children,[16] in Japan is expected.

References

1. Barnard CN. A human cardiac transplant: An interim report of a successful operation performed at Groote Schuur Hospital, Cape Town. *S Afr Med J* 1967; 41: 1271–1274.
2. Cooley DA, Bloodwell RD, Hallman GL, Nora JJ, Harrison GM, Leachman RD. Organ transplantation for advanced cardiopulmonary disease. *Ann Thorac Surg* 1969; 8: 30–46.
3. Caves PK, Stinson EB, Billingham ME, Shumway NE. Serial transvenous biopsy of the transplanted human heart: Improved management of acute rejection episodes. *Lancet* 1974; 1: 821–826.
4. Taylor DO, Edwards LB, Aurora P, Christies JD, Dobbels F, Kirk R, et al. Registry of the international society for heart and lung transplantation: Twenty-fifth official adult heart transplant report 2008. *J Heart Lung Transplant* 2008; 27: 943–956.
5. Lower R, Stofer RC, Shumway NE. Homovital transplantation of the heart. *J Thorac Cardiovasc Surg* 1961; 41: 196–204.
6. Kitamura S, Nakatani T, Bando K, Sasako Y, Kobayashi J, Yagihara T. Modification of bicaval anastomosis technique for orthotopic heart transplantation. *Ann Thorac Surg* 2001; 72: 1405–1406.
7. Imanaka H, Nakatani T, Kitamura S. Complications and problems of acute care in patient undergoing heart transplantation. *Kyobugeka* 2007; 60: 958–962 (in Japanese).
8. Billingham ME, Cary NR, Hammond ME, Kemnitz J, Marboe C, McCallister HA, et al. A working formulation for the standardization of nomenclature in the diagnosis of heart transplantation and lung rejection: Heart rejection study group. *J Heart Lung Transplant* 1990; 9: 587–593.
9. Wada K, Takeda M, Ueda T, Ochi H, Kotake T, Morishita H, et al. Relationship between acute rejection and cyclosporine or mycophenolic acid levels in Japanese heart transplantation. *Circ J* 2007; 71: 289–293.
10. Wada K, Takeda M, Kotake T, Ochi H, Morishita H, Komamura K, et al. Limited sampling strategy for mycophenolic acid in Japanese heart transplant recipients: Comparison of cyclosporin and tacrolimus treatment. *Circ J* 2007; 71: 1022–1028.
11. Kobashigawa J, Mehr M, West L, Kerman R, George J, Rose M, et al. Report from a consensus conference on the sensitized patient awaiting heart transplantation. *J Heart Lung Transplant* 2009; 28: 213–225.
12. Zuckermann A, Manito N, Epailly E, Fiane A, Bara C, Delgado JF, et al. Multidisciplinary insights on clinical guidance for the use of proliferation signal inhibitors in heart transplantation. *J Heart Lung Transplant* 2008; 27: 141–149.
13. The Japanese Society for Heart Transplantation. The registry report of Japanese heart transplantation 2008. *Ishoku* 2008; 43: 470–473 (in Japanese).
14. Matsuda H, Fukushima N, Sawa Y, Nishimura M, Matsumiya G, Shirakura R. First brain dead donor heart transplantation under new legislation in Japan. *J Jpn Thorac Cardiovasc Surg* 1999; 47: 499–505.
15. Kitamura S, Nakatani T, Yagihara T, Sasako Y, Kobayashi J, Bando K, et al. Cardiac transplantation under new legislation for organ transplantation in Japan: Report of two cases. *Jpn Circ J* 2000; 64: 333–339.
16. Kobayashi N, Ono Y, Tsukano S, Yazaki S, Yamada O, Echigo S, et al. Outcome of pediatric candidates for orthotopic heart transplantation at National Cardiovascular Center in Japan. *Pediatr Cardiol Card Surg* 2008; 24: 628–635 (in Japanese).

Body Mass Index is a Useful Predictor of Prognosis After Left Ventricular Assist System Implantation

Akiko Mano, MD, PhD,[a] Kiyoharu Fujita,[b] Kaori Uenomachi,[b] Keiichi Kazama,[b] Mayumi Katabuchi, RN,[b] Kyoichi Wada, BS,[b] Nobue Terakawa, BS,[b] Koji Arai,[b] Yumiko Hori, RN,[b] Syuji Hashimoto,[c] Takeshi Nakatani, MD, PhD,[d] and Soichiro Kitamura, MD, PhD[c]

Background: The obesity paradox has recently attracted considerable interest in the study of many diseases. In this investigation we examine the relationship between body mass index (BMI) and prognosis after left ventricular assist system (LVAS) implantation.

Methods: We measured the BMI of 64 patients 3 months after LVAS implantation for end-stage heart failure. The patients were classified according to BMI into Group A (BMI <16 kg/m^2), Group B (BMI 16 to 18.4 kg/m^2) or Group C (BMI ≥18.5 kg/m^2). We compared the prognosis among these three groups after a mean follow-up period of 583 days.

Results: Seven patients were weaned from their LVAS, 24 received heart transplantation, 25 died on the transplant waiting list, and 8 remain on the list. Long-term (>1 year) mortality was significantly higher in Group A than in Groups B and C (59% vs 40% and 18%, respectively; $p < 0.05$). The incidence of sepsis was also significantly higher in Group A than in Groups B and C (68% vs 45% and 32%, respectively; $p < 0.05$). After multivariate adjustment, BMI <16 kg/m^2 (hazard ratio [HR] 14.9; 95% confidence interval [CI] 2.61 to 86.0; $p < 0.01$) and levels of C-reactive protein (HR 1.56; 95% CI 1.15 to 2.13; $p < 0.01$) were independent predictors of mortality.

Conclusions: A lower BMI indicated a poor prognosis, as well as a higher incidence of a fatal complication, sepsis, after LVAS implantation. Control of BMI could be an effective way to improve management of patients with LVAS. J Heart Lung Transplant 2009;28:428–33. Copyright © 2009 by the International Society for Heart and Lung Transplantation.

Obesity is recognized as a risk factor for many diseases.[1] Obesity is associated with diabetes, hypertension, hyperlipidemia and other disorders, collectively known as the metabolic syndrome,[2-4] believed to increase mortality rates. However, recent studies have demonstrated that being underweight is can be a disadvantage. Flegal et al reported that overweight status is associated with a significantly decreased mortality from non-cancer, non-cardiovascular (CVD) causes, but it is not linked to cancer or CVD mortality.[5] They also showed that obesity increases the incidence of diabetes, kidney disease, obesity-related cancer and CVD mortality, but decreases mortality rates due to other cancers and non-cancer and non-CVD causes. Furthermore, although a higher body mass index (BMI) increases CVD,[6,7] many studies have revealed that BMI is inversely associated with mortality in heart failure.[8-10] This obesity paradox is evident in acute and chronic heart failure and has thus received considerable focus.[9,11,12]

The left ventricular assist system (LVAS) is a powerful circulatory support device that is very effective for patients with end-stage heart failure.[13] The LVAS can improve hemodynamic disturbance and organ dysfunction, and can generally maintain patient stability. Deteriorated cardiac function is almost fully compensated after LVAS implantation, except in cases of severe right heart failure. Most patients with LVAS are supported until a suitable donor heart becomes available. Several investigators have reported a higher risk of mortality after heart transplantation among both morbidly obese and cachectic patients.[14-16] In a study of pediatric heart transplant patients, Rossano et al demonstrated that being underweight (<5th percentile) at transplant was an independent predictor of decreased graft survival, although overweight patients showed similar graft survival compared with normal-weight patients.[17] It remains unknown, however, whether BMI influences the mortality of patients supported with LVAS. Herein we

From the [a]Department of Emergency and Critical Care Medicine, Tokushima University, Tokushima City, Tokushima, Japan; and the [b]Nutritional Support Team and Departments of [c]Physiology, [d]Organ Transplantation and [e]Cardiovascular Surgery, National Cardiovascular Center, Osaka, Japan.

Submitted August 19, 2008; revised November 26, 2008; accepted December 29, 2008.

Reprint requests: Akiko Mano, MD, Department of Emergency and Critical Care Medicine, Tokushima University, 2-50-1 Kuramoto-cho, Tokushima City, Tokushima 770-8503, Japan. Telephone: +81-88-633-9347. Fax: +81-88-633-9339. E-mail: akkmano1972@kve.biglobe.ne.jp

 1053-2498/09/$-see front matter. doi:10.1016/j.healun.2008.12.020

investigate the relationship between BMI and the prognosis of patients with LVAS.

METHODS

Patient Population

Eighty-three patients underwent LVAS implantation for end-stage heart failure at our institution between April 1994 and December 2006. All patients were diagnosed with New York Heart Association Class IV heart failure at the time of LVAS insertion and were supported with intravenous inotropic agents. Of these, we enrolled 64 patients (43 males, 21 females; age 8 to 58 years), whose BMI could be measured 3 months after LVAS implantation. Excluded patients were as follows: 3 patients underwent LVAS explantation (2 for heart transplantation and 1 for restoration of natural heart function) within 3 months; 11 patients died within 3 months; and 5 patients could not have BMI calculated at 3 months after implantation. We used BMI calculated at 3 months after implantation because a pre-implant BMI would result in overestimation due to fluid retention, and patients have usually recovered from surgical invasion and are stabilized by 3 months after operation.

The etiology of heart failure included dilated cardiomyopathy (DCM, $n = 52$), dilated phase of hypertrophic cardiomyopathy (dHCM, $n = 3$) or secondary cardiomyopathy (sarcoidosis, $n = 2$; myopathy, $n = 2$; drugs, $n = 2$; ischemia, $n = 3$). The Toyobo LVAS, HeartMate VE, Novacor and Evaheart devices were implanted into 55, 3, 4 and 2 patients, respectively. The patients were classified into Groups A, B and C according to BMI (kg/m^2) values of <16, 16 to 18.4 and ≥ 18.5, respectively. We retrospectively evaluated mortality and also investigated the incidence of infection, sepsis and cerebrovascular events (infarction and/or hemorrhage), which are the most frequent causes of death in patients on LVAS. Infection was defined as pus and/or exudate and/or abscess detected around LVAS cannulae, or infectious signs (local as well as systemic) confirmed by laboratory findings or by imaging. Sepsis was defined as fever ($\geq 38°C$) with microbes detected in blood cultures.

The study was approved by the institutional review board of the National Cardiovascular Center, and all patients provided written informed consent.

Statistical Analysis

Baseline characteristics of the patients across the three BMI groups were analyzed using the chi-square test for categorical variables and analysis of variance (ANOVA) for continuous variables. The incidence of mortality at 1 year after LVAS implantation and overall, as well as of infection, sepsis and cerebrovascular events were compared among the three groups using the chi-square test. We applied the Kaplan-Meier method to assess overall survival. Log-rank statistics were performed to assess the statistical significance of survival differences among the three groups. Unadjusted associations between mortality and several risk factors including BMI were investigated using the chi-square test. We evaluated whether different levels of BMI were independent predictors of mortality by using a multivariate Cox proportional hazards model adjusted for covariates considered to be prognostic predictors for congestive heart failure, including (CHF): age; gender; left ventricular diameter in diastole (LVDd); fractional shortening (FS); brain natriuretic peptide (BNP) level; and serum values for total bilirubin, creatine, hemoglobin, total protein, serum albumin and C-reactive protein (CRP). Statistical significance was defined by a 2-tailed $p < 0.05$. All analyses were performed using SPSS, version 2 for Windows (SPSS, Inc., Chicago, IL).

RESULTS

Patients' Characteristics

Table 1 summarizes the baseline (3 months after LVAS implantation), demographic and clinical characteristics of the study population. Patients in Group A were significantly younger than those in Groups B and C ($p < 0.05$). No statistical differences were identified among the three groups with regard to gender, DCM (percent), hemodynamic parameters and indicators of organ function. Furthermore, cardiac function evaluated by echocardiography, levels of BNP, as well as the ratio of patients supported with inotropic agents did not differ significantly among the groups. Levels of CRP were also similar among the groups. Levels of hemoglobin were significantly lower in Groups A and B than in Group C ($p < 0.05$), and albumin levels were significantly higher in Group C than in Groups A and B ($p < 0.01$).

We also evaluated the changes in BMI from pre-implant to 3 months after implantation. BMI decreased in all groups and the ratio (percent) of BMI changes did not differ significantly among the three groups.

The mean follow-up period was 583 days (Groups A, B and C: 485, 544 and 716 days, respectively). Seven patients were weaned from LVAS (Groups A, B and C: $n = 2$, 2 and 3, respectively), 24 underwent heart transplantation (Groups A, B and C: $n = 5$, 7 and 12, respectively), 25 died on the transplant waiting list (Groups A, B and C: $n = 13$, 8 and 4, respectively), and 8 remain on the list (Groups A, B and C: $n = 2$, 3 and 3, respectively).

Mortality After LVAS Implantation

Overall, 25 (39%) of 64 patients died on LVAS support. Figure 1A and B shows that the 1-year mortality rate tended to be lower in Group C than in Groups A and B (4.5% vs 18% and 20%, respectively), but the difference

Table 1. Baseline Patient Characteristics

	Group A ($N = 22$)	Group B ($N = 20$)	Group C ($N = 22$)	p-value
BMI (kg/m^2)	14.0 ± 1.2	17.6 ± 0.7	20.5 ± 2.6	<0.05[a]
ΔBMI	−10.5 ± 7.7	−5.8 ± 8.8	−6.3 ± 8.9	NS
Age (y)	29 ± 11	38 ± 12	38 ± 11	<0.05
Male (y)	50	70	82	NS
DCM (%)	82	85	82	NS
Inotropic agents	13.6	10	4.8	NS
SBP (mm Hg)	98 ± 8.8	98 ± 11	100 ± 9.6	NS
HR (bpm)	86 ± 15	87 ± 18	82 ± 16	NS
Dd (mm)	55 ± 14	62 ± 14	62 ± 15	NS
FS (%)	14 ± 10	13 ± 11	12 ± 11	NS
BNP (pg/ml)	454 ± 634	220 ± 208	191 ± 222	NS
Hemoglobin (g/dl)	10.1 ± 1.4	10.4 ± 1.2	11.2 ± 1.4	<0.05
Total bilirubin (mg/dl)	0.9 ± 0.4	0.8 ± 0.4	0.8 ± 0.4	NS
Creatine (mg/dl)	0.6 ±v0.3	0.7 ± 0.2	0.8 ± 0.4	NS
Total protein (g/dl)	6.7 ± 0.7	6.8 ± 0.6	6.9 ± 0.6	NS
Albumin (g/dl)	3.7 ± 0.4	3.6 ± 0.3	4.0 ± 0.2	<0.01
T-chol (mg/dl)	167 ± 28	161 ± 32	188 ± 36	NS
CRP (mg/dl)	2.0 ± 3.8	1.5 ± 2.1	0.8 ± 0.8	NS

Groups A, B and C: BMI <16 kg/m^2, 16 to 18.4 kg/m^2 and ≥18.5 kg/m^2, respectively. BMI, body mass index; ΔBMI, changes in BMI from pre-implantation to 3 months post-implantation; DCM, dilated cardiomyopathy; SBP, systolic blood pressure; HR, heart rate; Dd, left ventricular diameter in diastole; FS, fractional shortening; BNP, brain natriuretic peptide; T-chol, total cholesterol; CRP, C-reactive protein; NS, not statistically significant.

was not statistically significant. On the other hand, overall mortality was significantly lower in Group C than in Groups A or B (18% vs 59% and 40%, respectively; $p < 0.05$). Short- and long-term mortality rates did not differ significantly between Groups A and B. Figure 2 shows survival curves for the three groups. Log-rank statistics also generated the same results.

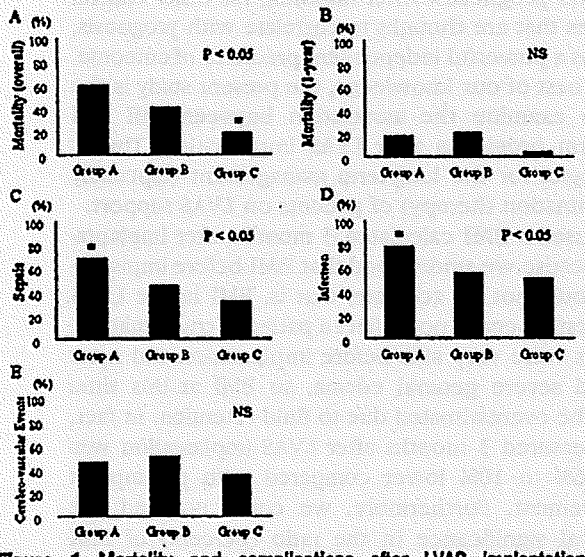

Figure 1. Mortality and complications after LVAS implantation. (A) Overall mortality; *$p < 0.05$ vs Groups A or B. (B) One-year mortality. (C) Incidence of sepsis; *$p < 0.05$ vs Groups B or C. (D) Incidence of infection; *$p < 0.05$ vs Groups B or C. (E) Incidence of cerebrovascular events. LVAS, left ventricular assist system.

Complications After LVAS Implantation

Figure 1C–E shows the actual state of complications while on LVAS support. The incidence of infection (mostly bacterial and around cannulae) was significantly higher in Group A than in Groups B and C (77% vs 55% and 50%, respectively; $p < 0.05$). The incidence of sepsis was also significantly higher in Group A than in Groups B and C (68% vs 45% and 32%, respectively; $p < 0.05$). The percentage of patients who developed cerebrovascular events did not differ significantly among the three groups (Group A vs B and C: 45% vs 50% and 30%).

Predictors of Overall Mortality After LVAS Implantation

Table 2 shows the univariate predictors of prognosis derived from Cox regression analysis. BMI was closely associated with mortality. The risk of death was significantly higher in Group A than in Group C (hazard ratio [HR] 3.25, 95% confidence interval [CI] 1.25 to 8.42, $p < 0.05$). Group B also had a higher risk of death compared with Group C, but the difference did not reach statistical significance (HR 2.22, 95% CI 0.78 to 6.20). Other variables that correlated with mortality were BNP level ≥100 pg/ml (HR 3.98, 95% CI 1.33 to 11.9, $p < 0.05$), hemoglobin <10 g/dl (HR 2.19, 95% CI 1.18 to 4.08, $p < 0.05$) and creatinine ≥1.2 mg/dl (HR 1.98, 95% CI 1.03 to 3.81, $p < 0.05$). Table 3 shows the results of multivariate Cox regression analysis. After adjusting for various characteristics of the patients, BMI was an independent predictor of mortality. Patients in Group A were at a significantly higher risk of death